DOKUZ EYLÜL UNIVERSITY
GRADUATE SCHOOL OF NATURAL AND APPLIED SCIENCES

LOW VELOCITY IMPACT AND COMPRESSION-AFTER IMPACT BEHAVIORS OF ADVANCED COMPOSITES AT LOW TEMPERATURES

by
Samet KIYIK

January, 2021
İZMİR

LOW VELOCITY IMPACT AND COMPRESSION-AFTER IMPACT BEHAVIORS OF ADVANCED COMPOSITES AT LOW TEMPERATURES

A Thesis Submitted to the
Graduate School of Natural and Applied Sciences of Dokuz Eylül University
In Partial Fulfillment of the Requirements for the Degree of Master of Science
in Mechanical Engineering, Mechanics Program

by
Samet KIYIK

January, 2021
İZMİR

M.Sc THESIS EXAMINATION RESULT FORM

We have read the thesis entitled **"LOW VELOCITY IMPACT AND COMPRESSION-AFTER IMPACT BEHAVIORS OF ADVANCED COMPOSITES AT LOW TEMPERATURES"** completed by **SAMET KIYIK** under supervision of **PROF. DR. RAMAZAN KARAKUZU** and we certify that in our opinion it is fully adequate, in scope and in quality, as a thesis for degree of Master of Science.

Prof. Dr. Ramazan KARAKUZU

Supervisor

Prof. Dr. Kutlay SEVER

(Jury Member)

Assoc. Prof. Dr. Okan ÖZDEMİR

(Jury Member)

Prof. Dr. Özgür ÖZÇELİK

Director

Graduate School of Natural and Applied Sciences

ACKNOWLEDGMENTS

Throughout the writing of this thesis I have received a great deal of support and assitance. I would like to thank my supervisor Prof. Dr. Ramazan KARAKUZU, who has always helped me with his valuable knowledge and guided me during my studies for three years.

I would like to thank my colleague Halis Kandaş, who helped me as much as he could and supported me in every aspect of the laboratory studies during my thesis.

Finally, I would like to thank my family for their wise counsel. In addition, I could not have completed this thesis without the support of my parents.

Samet KIYIK

LOW VELOCITY IMPACT AND COMPRESSION-AFTER IMPACT BEHAVIORS OF ADVANCED COMPOSITES AT LOW TEMPERATURES

ABSTRACT

Composite materials are the general name given to materials created by a combination of two or more materials. Thermoset composites are resistant to high temperatures due to the strong covalent bonds between their chemical structures and are therefore used in many areas such as aviation, space and automobiles. Therefore, in this study, S2 glass / epoxy composite material was chosen to examine the low velocity impact and compression-after impact (CAI) behaviors.

In this study, S2 glass/epoxy laminated composites were produced with a vacuum assisted resin infusion molding (VARIM) method. After that samples were prepared in dimensions of 100 mmx150 mm. First, impact tests were conducted at -50°C, -25°C and 20°C temperatures and 30 J, 40 J and 50 J impact energies for two different material thicknesses of 2.72 mm and 3.02 mm. Impact tests were performed by CEAST 9350 Fractovis Plus impact test machine. Then, impact behaviors were examined with the help of contact force-time and energy-time graphs. Impact damage photos of samples were given in figures. After impact tests, Compression-After Impact (CAI) test was applied to the samples at 20°C by Universal Shimadzu machine and a Boeing CAI fixture (ASTM D 7137) test apparatus. The effects of thickness, temperature and impact energy on CAI strength were examined. Impact and CAI damage photos of samples were also examined by visual inspection.

Keywords: Low velocity impact, compression-after impact, vacuum assisted resin infusion molding, S2 glass/epoxy

İLERİ KOMPOZİTLERİN DÜŞÜK SICAKLIKLARDA DÜŞÜK HIZLI DARBE VE DARBE SONRASI BASI DAVRANIŞLARI

ÖZ

Kompozit malzemeler, iki veya daha fazla malzemenin bir kombinasyonu ile oluşturulan malzemelere verilen genel addır. Termoset kompozitler kimyasal yapılarının arasındaki güçlü kovalent bağlardan ötürü yüksek sıcaklıklara dayanıklılardır ve bu sayede havacılık, uzay ve otomobil gibi birçok alanda kullanılmaktadırlar. Bu yüzden bu çalışmada S2 cam/epoksi kompozit malzemesi seçilerek, düşük hızlı darbe ve darbe sonrası bası (CAI) davranışları incelenmiştir.

Bu çalışmada S2 cam/epoksi kompozit malzemeleri vakum destekli reçine infüzyon kalıplama (VARIM) yöntemiyle üretilmiştir. Daha sonra 100 mmx150 mm boyutlarında numuneler hazırlanmıştır. İki farklı kalınlıkta (2,72 ve 3,02 mm) üretilen numunelere önce -50 °C, -25 °C ve 20 °C sıcaklıklarda ve 30 J, 40 J ve 50 J darbe enerjilerinde darbe testleri uygulanmıştır. Darbe testleri CEAST 9350 Fractovis Plus darbe test makinesi yardımıyla yapılmıştır. Daha sonra temas kuvveti-zaman ve enerji-zaman grafikleri yardımıyla darbe davranışları incelenmiştir. Darbe testleri sonrası numunelere 20 °C de Universal Shimadzu makinesi ile Boeing CAI bağlama (ASTM D 7137) test aparatı kullanılarak CAI testleri uygulanmıştır. Kalınlık, sıcaklık ve darbe enerjisinin bası dayanımına etkileri incelenmiştir. Ayrıca numunelerin darbe ve CAI hasar fotoğrafları görsel olarak incelenmiştir.

Anahtar kelimeler: Düşük hızlı darbe, darbe sonrası bası, vakum destekli reçine infüzyonu kalıplama, S2 cam/epoksi

CONTENTS

Page

M.Sc THESIS EXAMINATION RESULT FORM ii

ACKNOWLEDGMENTS iii

ABSTRACT iv

ÖZ v

LIST OF FIGURES viii

LIST OF TABLES x

CHAPTER ONE – INTRODUCTION 1

CHAPTER TWO – COMPOSITE MATERIALS 11

2.1 Matrix Materials 11

2.1.1 Metal Matrices 12

2.1.2 Ceramic Matrices 12

2.1.3 Polymer Matrices 13

2.1.3.1 Thermoset and Thermoplastic Polymers 14

2.2 Reinforcement Materials 16

2.2.1 Fibers 16

2.2.1.1 Glass Fibers 17

2.2.1.2 Aramid Fibers 19

2.2.1.3 Graphite Fibers 20

2.2.2 Particles and Whiskers 21

2.3 Laminated Composites 21

CHAPTER THREE – MATERIALS AND METHOD 23

3.1 Production of Composite Materials 23

3.2 Impact Test 26

3.3 Compression-After Impact (CAI) Test 27

CHAPTER FOUR – RESULTS AND DISCUSSIONS **28**

4.1 Impact Results 28
4.1.1 Contact Force 29
4.1.2 Absorbed Energy 39
4.1.3 Impact Damage 43
4.2 CAI Results 47
4.2.1 CAI Strength 48
4.2.2 CAI Damage 51

CHAPTER FIVE – CONCLUSION **58**

REFERENCES **61**

LIST OF FIGURES

Page

Figure 2.1 Polymer, metal matrix and ceramic composite differences 13
Figure 2.2 Thermoset and thermoplastic structures 14
Figure 2.3 Performance comparison of different polymer matrices 16
Figure 2.4 Shows the specific tensile strength and modulus graph for commonly used fibers 17
Figure 2.5 Comparison of stress-strain curves for high-strength fibers 19
Figure 2.6 Crystal structure of graphite fibers 21
Figure 2.7 Schematic analysis of laminated composites 22
Figure 3.1 Shows the schematic representation of the VARIM process 24
Figure 3.2 a) S2 glass fabrics on mold release agent on, b) peel ply is placed on S2 glass fabrics, c) resin dispersant placed on the peel ply, d) whole system is covered with vacuum bag.. 25
Figure 3.3 The water saw for cutting sample 25
Figure 3.4 a) CEAST Fractovis Plus impact test machine, b) test specimen, c) liquid nitrogen tank 26
Figure 3.5 a) Shimadzu AG-X tension/compression testing machine with compression after impact (CAI) apparatus, b) CAI test apparatus 27
Figure 4.1 Force-time graph of impact test group made at 3.02mm thickness at 20°C and 30J energy 30
Figure 4.2 Contact force-time graphs according to the impact energy for different temperatures and thickness .... .31
Figure 4.3 Contact force-time graphs according to the temperature for different impact energy and thicknesses... .33
Figure 4.4 Contact force-time graphs according to the thickness for different impact energy and temperatures 34
Figure 4.5 Maximum contact force change due to energy change of composites with a) 2.72mm and b) 3.02mm thicknesses in low velocity impact test 35
Figure 4.6 Maximum contact force change due to temperature change of composites with a) 2.72mm and b) 3.02mm thicknesses... 37
Figure 4.7 Maximum contact force change due to thickness change of composites at

a) 20°C, b) -25°C and c)-50°C temperatures 39
Figure 4.8 Definition of impact energy, absorbed energy and elastic energy on energy-time graph.. 40
Figure 4.9 Energy-time graphs depending on energy change.................................. 41
Figure 4.10 Energy-time graphs due to temperature change 42
Figure 4.11 Energy-time graphs depending on the thickness of composite materials for different impact energy and temperature 43
Figure 4.12 Impact damages types of S2/glass epoxy samples with 2.72mm and 3.02mm thicknesses at different impact energies at 20°C 45
Figure 4.13 Impact damage types of S2/glass epoxy samples with 2.72mm and 3.02mm thicknesses at -25°C at different impact energies.................. 45
Figure 4.14 Impact damage types of S2/glass epoxy samples with 2.72mm and 3.02mm thicknesses at -50°C at different impact energies.................. 46
Figure 4.15 Impact damage area on the back face after low velocity impact test applied at different impact energy and temperature in samples with a) 2.72mm and b) 3.02mm thicknesses 47
Figure 4.16 CAI test results of samples with 2.72mm thickness subjected to impact at 20°C temperature and 30J energy values 48
Figure 4.17 Variation of CAI strength at a) 2.72mm and b) 3.02mm thicknesses depending on temperature and energy changes 50
Figure 4.18 Damage after low velocity impact test and CAI test of S2 glass/epoxy samples with 2.72mm thickness at 20°C and different impact energies …52
Figure 4.19 Damage after low velocity impact test and CAI test of S2 glass/epoxy samples with 3.02mm thickness at 20°C and different impact energies….53
Figure 4.20 Damage after low velocity impact test and CAI test of S2 glass/epoxy samples with 2.72mm thickness at -25°C and different impact energies 54
Figure 4.21 Damage after low velocity impact test and CAI test of S2 glass/epoxy samples with 3.02mm thickness at -25°C and different impact energies 55
Figure 4.22 Damage after low velocity impact test and CAI test of S2 glass/epoxy samples with 2.72mm thickness at -50°C and different impact energies 56
Figure 4.23 Damage after low velocity impact test and CAI test of S2 glass/epoxy samples with 3.02mm thickness at -50°C and different impact energies 57

LIST OF TABLES

Page

Table 2.1 E-glass and S-glass chemical compositions 19
Table 4.1 Low velocity impact test results for different temperatures and energies . 29
Table 4.2 Maximum forces and CAI strengths of CAI test for 2.72mm and 3.02mm thicknesses specimens subjected to low velocity impact test at different temperatures and energies 49

CHAPTER ONE
INTRODUCTION

The classification of composite materials are divided into two. The first is the classification according to the matrix material type. Composite materials by type of matrix material; can be listed as metal, ceramic and polymer matrix. Secondly, composite materials are classified according to the shape and placement of the reinforcing elements. According to this classification, composite materials; they are divided into four as fiber composites, layered composites, particulate composites and mixed composites.

As can be seen, composites have many classification types. Today, the most widely used type of these composite materials is polymer matrix thermoset and thermoplastic. The matrix material used in this study is epoxy thermoset plastic material. According to the type of hardener used in the epoxy matrix material, the properties of the composite material also change. Since composites with excellent mechanical properties can be obtained with glass and carbon fiber, such composite materials have a very common use in the aerospace, aviation and marine industries. Disadvantages of epoxy, high cost, unfavorable properties arising in case of wrong mixing ratio (thus it is extremely important and meticulous to prepare the correct mixing ratio), and finally as they are harmful for skin, during the production of equipment such as protective clothing and gloves correct mixing ratio is essential and should be done in appropriate way.

Nowadays as the usage areas of composite materials are increasing day by day, researchers and scientists have done many studies on these materials. Some of these studies are as follows:

Composite structures are widely used in the automobile, marine and aircraft industries and these materials are inevitable to undergo low-velocity impacts or different temperatures during the assembly stages and throughout their service life. Therefore, theoretically calculated material properties may change due to exposure to these low impacts or temperatures. Khashaba & Othman (2017) applied a low-velocity impact between 15J and 85J on woven carbon reinforced epoxy (CFRE) composite material. They also repeated these impacts at room temperatures, 50°C and 75°C. In experiments, it was observed that the temperature causes to perforation at 75°C due to the softening of the epoxy matrix. At the same time, it was observed that there was no perforation at any temperature in the 15J and 35J impact energies. Körbelin, Derra & Fiedler (2018) examined the low velocity impact responses of temperature and impact energy changes in CFRP samples in their study. While the thickness of quasi-isotropic laminate samples is 4.1mm, the impact energy values are 8J, 15J, 18J and 21J. The temperature values selected in the experiments are 20°C, 50°C and 80°C. As a result of the tests, it was observed that the delamination area in the samples decreased as the temperature increased. Karakuzu, Erbil & Aktas (2010) examined the effects of impact energy, impactor mass and impact velocity on maximum contact force, maximum deflection, contact time, absorbed energy, and overall damage area in their study on glass/epoxy laminated composites. In the study, composites plates were selected in the sequence $[0°/30°/60°/90°]_s$. In the results, low impactor mass and higher velocity were found to be less than the damage area, higher impactor mass and lower velocity test setup. In experiments using higher impactor mass, contact time is higher than in lower impactor mass experiments. Reis et al. (2012) examined the behavior of the impact response of Kevlar/filled epoxy matrix with two different filler materials. Cloisite 30B and cork powder were used as filler. As a result of the experiments, it has been seen that the nanoclays filling material gives better impact response results. Reis et al. (2013) examined the impact responses of Kevlar/epoxy laminate composites with different nanoclay Cloisite 30B supplements. 6%, 3% and 1.5% ratios were chosen as nanoclay supplements. As a result of the tests, it was seen that 6% nanoclay reinforced Kevlar/epoxy laminate composites had the best impact response results. Aryal et al. (2019) examined the low velocity impact responses of carbon fiber reinforced laminates and sandwich structures. Two different test setups were prepared as the impact energy between 17.13J and 154.18J. In the first experimental setup, the same impactor mass and velocity were selected with different impact energies, while in the second experimental setup, the same impact energy and different impactor mass and velocity were selected. As a result, the increase in impactor mass and localized damage patterns seem similar, but it was seen that it caused a higher core damage. Aslan, Karakuzu & Okutan (2003) examined the low velocity impact response of the E-glass/epoxy $[0/90/0/90]_s$ laminated oriented cross-ply composite. In the impact test, 135g and 2600g impactor mass and impact velocity of 3m/s were selected. Composite samples have been selected in three different dimensions. As a result of the tests, it was seen that when the width of the samples was reduced, contact duration increased. The highest value of maximum impact force was found in 150mmX100mm composite sample, while the highest delamination area was found in the same samples. Aktaş et al. (2009) analyzed the impact responses on unidirectional glass/epoxy composite laminates. The results of samples with two different $[0/90/0/90]_s$ and $[0/90/+45/-45]_s$ stacking sequences were compared. The penetration threshold $[0/90/+45/-45]_s$ was lower in the samples. At impact energies less than 25J, the main damage was matrix cracks and delamination, while at higher impact energies fiber failures became a more dominant damage mode. İçten & Karakuzu (2008) produced four different loose and tight plain weave layers, low, and high curing pressure in their studies on E-glass/epoxy laminated composites. In the results, it has been seen that the weaving density has a significant effect on the impact response. It has been observed that the loose woven composites have a higher perforation threshold. Likewise, it has been observed that composites produced with low pressured curing have a higher perforation threshold than composites produced with high pressured. Atas & Sayman (2008) applied a low velocity impact test between 4J and 45J to the E-glass/epoxy composites in their studies. As a result of the studies, they showed that the damage process of the samples can be reconstructed by comparing the energy profile diagram, images of damaged samples and contact force-deflection graphics. Kazemi et al. (2021) examined the effects of different fiber type and matrix type on low velocity impact tests. In the tests, woven ultra-high molecular weight polyethylene (UHMWPE) fabric and woven carbon fabric were used for the samples, while composites with different structures were produced using the newly developed thermoplastic Elium 188 and two different thermosets Epolam 5015 and Sikafloor 156 as resin. Five different energies were used as impact energy as 40J, 33J, 20J, 15J and 10J. As a result, compared to UHMWPE fabrics in carbon fabrics, the structural loss of the system was reduced by 47% and the absorbed energy was reduced by 18%.

When thermoplastic resins and thermoset resins are compared, it is seen that thermoplastics reduce contact force by 14%, absorbed energy by 48% and structural loss by 200%. Finally, it has shown that Elium, which is a thermoplastic resin, is a very important resin with its ability to produce at room temperature, eliminate residual thermal stress, high production efficiency, recyclability and reduce production costs compared to thermosets.

Since composite materials are used in different conditions and sometimes at extreme temperatures, many studies have been done on the effect of temperature in composites. In their research, Galvez et al. (2016) applied a high-velocity impact on the carbon/epoxy composites at very low temperatures. For the shots made with 7.62mm caliber bullets, the projectile speed reached between 200m/s and 600m/s. In the experiments, it was concluded that the carbon/epoxy composite material has a much more fragile structure at very low temperatures and under dynamic loading. Reddy et al. (2019) studied the behavior of E-glass/epoxy composite material when exposed to different laminate thicknesses and low-velocity impact at different temperatures. In the research, a wide temperature range -20°C, 25°C and 100°C was chosen. As for the impact energies 50J, 100J and 150J are selected. As a result, it was found that as the thickness of the lamina increases, the strength of the material increases, but at the same time, the effect of temperature on the perforation threshold energy become more important due to the increase of lamina hardness at low temperatures as the thickness of lamina increases. Taraghi, Fereidon & Taheri-Behrooz (2014) studied the behavior of kevlar/epoxy laminated composites enchanced with different weight percentages of multi-walled carbon nanotubes (MWCNTs) with different temperatures (27°C and -40°C) and 45 J impact energy. They are measured absorbed energy, velocity and deflection. As a result, it was founded that MWCNTs composites have improved impact response and reduced area of damage as temperature decreases. Icten et al. (2009) examined the low velocity impact responses of glass/epoxy laminated composites at 20°C, -20°C and -60°C. Impact energy has been selected between 5J and 70J. As a result of the experiment, it was seen that the perforation threshold increased as the temperature decreased. While the impact energy is 20J, the impact response and damage tolerance is almost the same at all temperatures. Rio et al. (2005) examined the low temperature and low velocity impact response of carbon fiber epoxy laminated composites. In that work, the temperature was chosen as 20°C, -60°C and -150°C. Four different stacking sequences selected unidirectional, cross-ply, quasi-isotropic and woven were used as laminates samples. As a result, the choice of stacking sequences and fiber reinforcement architecture was found to be of major importance in CFRP composites. Sorrentino et al. (2017) examined the static and low velocity impact responses of poly-based thermoplastic composites (PEN) at different temperatures. Four different Vectran, carbon, basalt and Twaron fibers were selected as matrix reinforced in the study. For the test temperatures 100°C, 60°C and 20°C have been chosen. As a result of the tests, PEN/basalt composites gave the best performance results, and it was observed that PEN/Twaron composite material gave the second-best results. Aktaş, Karakuzu & İçten (2011) produced the E-glass/epoxy composite material in three different laminated form in their study. Laminate composites produced in the form of $[0]_8$, $[0/90/+45/-45]_s$ and $[0/90/0/90]_s$ are 3mm thickness. 3DIMPACT was used for numerical analysis in the study, which was conducted by performing experimental and numerical analysis. Impact tests were conducted at five different temperatures in the studies. In the impact tests performed at 20°C, 40°C, 60°C, 80°C and 100°C, it was observed that the maximum contact force decreased as the stiffness of the samples decreased as the temperature increased. It has been observed that as the impact energy increases, the maximum contact force and the deflection also increase. Aktaş, Karakuzu & Icten (2010) investigated the impact response of the samples in their studies on E-glass/epoxy samples. Two different stacking sequences were used in studies performed at three different temperatures (20°C, 60°C and 100°C). The dimensions of the samples produced in 3mm thickness are 100mmX100mm. As a result of their work, they observed that the absorbed energy of the samples increased as the temperature increased. Finally, it was observed that the temperature increase, increased perforation threshold.

Compression after impact (CAI) is a method used to determine the residual compressive strength of the composite material after impact loading. Researchers have done many studies because of the application areas where compressive strength of composite material is important. Aktaş, Karakuzu & Arman (2009) applied different impact energies to two different laminate orientation glass/epoxy composite materials at room temperature and high temperatures. After these tests, they investigated the CAI resistance of composite materials with different laminate orientation. As a result of the tests, they concluded that the effect of temperature is very important in both laminate orientation. While 100°C temperature decreased the CAI resistance, the decrease was found to be the lowest at 20°C room temperature. Bai et al. (2019) carried out a low-velocity impact test to the foam-core sandwich (FCS) panels, and then conducted a CAI test to these panels. The test results showed that as the impact energy increases, CAI strength decreases. Tuo et al. (2019) examined the failure and damage mechanism of unidirectional carbon/epoxy prepregs by numerical and experimental methods applying different impact energies and CAI loading. The test results, just like previous studies, showed that as the impact energy increases, CAI strength decreases in both numerical and experimental results. Ouyang and other (2020) have developed a model for composite structures to find CAI strength faster and more efficiently. This simulation model which is created by the ABAQUS program has been shown to give accurate results compared to other CAI studies in the literature. Iqbal et al. (2009) investigated the effects of nanoclay ratio in carbon fiber/epoxy laminated composites on low velocity impact response and post-impact CAI tests. As a result of the tests, it has been seen that CFRP composites with nanoclay have smaller damage area, higher impact damage resistance and higher residual strength. Samples with a nanoclay ratio of 3% gave the best results. Sun & Hallett (2018) used two similar CFRP quasi isotropic laminate composites $[45_2/90_2/0_2/-45_2]_{2s}$ and $[45/90/0/-45]_{4s}$. CAI tests were applied after low velocity impact. As a result of the experiments, it has been observed that Ss laminate composites have higher impact resistance and CAI strength. Yang et al. (2021) applied low velocity impact and then compression after impact tests on CFRP composites. In the low velocity impact tests, impact energies of 20J, 33J and 40J were selected, here two different impactor diameters of 33J energy were selected. At the same time, the finite element models of the samples were examined. As a result of the tests carried out, CAI strength increases as the impactor diameter decreases, at the same time, CAI strength decreases as the impact energy increases. Liu, Falzon & Tan (2018) examined the CAI strength of hybrid unidirectional woven carbon fiber composite material with finite element simulation and experimental tests. Two different composite lamina lay-ups were used in the tests. Considering the test results, it was seen that there was a small but measurable increase in the CAI strength of the samples with woven plies on the lamina surfaces, and this had a positive effect. Saez, Barbero & Navarro (2008) examined the compression after impact test results of two different (tape and woven) laminate carbon fiber composite materials at low temperatures. While the low velocity impact test was performed at room temperature, CAI tests were conducted at 20°C, -60°C and -150°C. As a result of the tests, CAI strength decreased as the temperature decreased in tape laminates. Likewise, as the impact energy increased in all test groups, CAI strength decreased. In the CAI tests performed at low temperatures in woven laminate composites, higher CAI strength was obtained than at room temperature. Alpyildiz et al. (2009) examined the results of samples for impact, compression, tensile and CAI tests in their studies on glass knitted fabrics composed of tuck stitches composites. In the study, the results of 1x1 rib knitted fabrics and full cardigan derivative knitted fabrics of glass fibers samples were compared with each other. According to the results, the damage caused by the impact load was observed in the full cardigan derivative fabric composites at higher impact energies. The CAI strength value is higher with full cardigan derivative fabric composites than 1x1 rib knitted fabrics composites. Salehi-Khojin et al. (2006) chose 8J, 15J and 25J as impact energy in their studies on Kevlar/fiberglass composite laminates, while they chose -50°C, 25°C, 70°C and 120°C as temperatures in low velocity impact tests. CAI tests were applied to the samples after low velocity impact tests in the study. Three different laminate constructions were selected in the study. The first one of the selected layers consisted of 8 fiberglass, the second one of 6 fiber glass and 2 Kevlar (on the top and bottom) and the last one of 6 fiberglass and 2 Kevlar (on the middle part). In the results, absorbed energy at low impact energies is almost constant and independent of temperature. As the impact energy increases, the absorbed energy change becomes more dependent on the temperature change. Looking at the results, elastic energy decreases with increasing temperature at all impact energy values. Maximum force impact increases with increasing energy and decreasing temperature. The highest value of CAI strength was found at room temperature. Safri, Sultan & Jawaid (2019) added sugar palm composite glass fiber in their study. In the study, after benzoylation procedures, the impact response and CAI values were examined. In the results, it was observed that there was an increase in the dynamical mechanical properties of sugar palm composites after benzoylation treatment. In low velocity tests, it has been observed that the more impact energy increases, the more severe damage occurs to the samples. Finally, it was observed that CAI strength decreased as the impact energy increased. Shah et al. (2021) compared the performance of thermoplastic and thermoset, which are two adhesion, by applying CAI test and finite element simulation to thermoplastic 3D fiber reinforced composite and resin infused thermoset 3D fiber reinforced composites after low velocity impact. In the tests, four different impact tests were applied at 25J, 50J, 75J and 100J energy. When the CAI strength-impact energy graph was drawn in the CAI tests applied after the impact tests, there was almost no change in CAI strength due to impact energy in samples produced with thermoplastic, while there was a noticeable decrease in CAI strength as the impact energy value increased in samples produced with thermoset. This situation was observed comfortably in the compressive load-displacement charts, as the impact energy increased, there was a big decrease in the samples produced with thermoset in compressive load. When buckling load is applied to samples produced with thermoplastic, there was less decrease in load compared to thermosets. As a result of the study, it has been observed that thermoplastic has a significantly superior damage tolerance compared to thermosets. The higher fracture toughness and higher-pressure ductility of thermoplastic have led to these results. Han et al. (2016) applied low velocity impact and compression after impact tests on four different laminate composites and compared the results with each other. In the tests where two different CCF300 and CCF800 carbon were used as fiber, epoxy and bismaleimide were used as resin. At the end of the tests, a finite element analysis was performed and compared with experimental analysis. As a result, epoxy matrix composite materials as resin gave better results in bismaleimide than matrix composite materials. A lower delamination area was formed at the same impact energies in epoxy resin matrix composites. When compared to fibers, CCF300 composites showed better tolerance performance against impact. In terms of CAI strength value, the results of epoxy resin composite materials gave better results than bismaleimide resin composites.

Depending on the thickness of the lamina in composites, the impact forces on the sample and the peak force vary in parameters such as maximum displacement and damage area. In this context, Reddy et al. (2019) applied impact energies between 50J and 150J by using 16mm hemispherical impactor for E-glass/epoxy composites with different lamina thickness. As a result of the tests, parameters such as peak force and maximum displacement were examined. Aslan, Karakuzu & Sayman (2002) analyzed the impact responses depending on the thickness of the E-glass/epoxy composites. The samples produced in three different sizes of 150mmx50mm, 150mmx100mm and 150mmx150mm also have two different 1.4mm and 2.8mm thicknesses. Impact tests were applied at speeds of 3, 2 and 1m/s. The results show that samples with larger width have higher peak force and lower contact time. Peak force was lower in thin plate samples. Delamination was higher in thin laminates than thick laminates. Mahesh, Joladarashi & Kulkarni (2020) produced jute/epoxy composite material in 6mm, 8mm and 10mm thickness. Later, they performed the low velocity impact tests at speeds of 2m/s, 4m/s, 6m/s and 8m/s. They used three different impactors as flat, conical and hemispherical in low velocity impact tests. As a result, the absorbed energy was the highest in the samples in the conical shaped impactor, while greater damage occurred in the flat shaped impactor. Bienias, Jakubczak & Dadej (2016) conducted a study on impact resistance by applying low velocity impact tests to aluminum/glass-epoxy composites. Two different 10J and 25J impact energy, room temperature impact tests were applied to composites produced in two different thicknesses of 1.5mm and 3.5mm. At the end of the tests, the accuracy of the results was investigated by performing a numerical study.

Generally, low temperatures or S2 glass/epoxy composite materials are not used in studies made on the effect of temperature. Today, it has been observed that there are some tests are applied at low temperature. For this reason, in this study, it is aimed to investigate the low temperature impact and compression after impact responses of S2 glass/epoxy composites. Composites with 2.72mm and 3.02mm thicknesses are produced and the samples are prepared in 100mmx150mm sizes. Low velocity impact tests are carried out at 20°C, -25°C and -50°C temperatures and 30J, 40J and 50J impact energies. Force-time and energy-time graphs are drawn and examined.

Afterwards, the CAI test was conducted to the samples at 20°C and finally the compression strength of the samples was examined by drawing CAI strength graphs.

CHAPTER TWO
COMPOSITE MATERIALS

Metals, ceramics, plastics and composite materials are often used in the field of engineering. Composite materials or shortened to composites are made by a combination of two or more materials which have different properties. Unlike the metallic alloys in composite materials, each material retains its physical, mechanical and chemical properties separately. As we mentioned earlier composites are made of constituent materials. Constituent materials can be divided into two category matrix as binder and reinforcement. Reinforcement materials can be supported and surrounded by help of the matrix materials. If it is necessary to list the duties of the matrix region, these are; To increase the toughness of the composite material, to prevent crack formation or to prevent its progress if cracks occur, to protect the fibers in the composite material from the conditions and impacts of the environment, to transmit the forces on the material to the fibers and to ensure its distribution properly. The reinforcing component in the composite material is responsible for carrying the loads on the material.

Composite materials have many advantages as well as some disadvantages. The advantages of composite materials can be listed as follows; High strength, high fracture toughness, high thermal properties, high wear resistance, low weight and high rigidity. The disadvantages of composite materials can be listed as follows; inherently difficult to recycle, high cost. Since composites are often constructed of different ply layers into a laminated structure delamination occurs between layers, cause to fracture, and cracking, complex production process than metal materials.

Composite materials contains matrix and reinforcement materials.

2.1 Matrix Materials

Matrix materials have very important applications such as keeping the fibers in the proper orientation and range and protecting them from abrasion and environmental effects (Campbell, 2010). In this classification, which is divided into three types according to the matrix material type, it is very important to choose the matrix material according to the area which will be used, because these three types of matrix material have advantages and disadvantages. Therefore, knowing the properties of metal, ceramic and polymer matrices is very important in making this choice.

2.1.1 Metal Matrices

Metal matrix composites have many advantages over normal metals. These advantages are high temperature resistance, higher strength, low thermal expansion coefficient, and also in some cases shows resistance to wear compared to metals. However, despite these many advantages, they are not preferred much because of their high costs (Campbell, 2010).

Metal matrix composites can be used with many reinforcing elements. Stiff boron and silicon carbide monofilament fibers have been used in aerospace studies. Aluminum is another reinforcing element which are the most used in commercial studies today as metal matrices. The resistance and lightness of aluminum to environmental effects made aluminum metal composites attractive (Campbell, 2010).

Determining how the manufacturing process of a metal matrix composite will be depends on many factors. The most important of these factors is undoubtedly the protection of reinforcement force and direction. It is very important to minimize damage to the reinforcement element due to chemical reactions that may occur between the matrix and the reinforcement element (Campbell, 2010).

2.1.2 Ceramic Matrices

Ceramics are materials with high thermal shock resistance, high temperature resistance, high hardness and corrosion resistance but at the same time, they are very fragile, and when cracks occur in this material due to low fracture toughness, the spread of this crack can occur quickly (Mallick, 2007).

In ceramic matrices, fibers, whiskers and particles are used to help increase toughness, but in metal and polymer matrices, these reinforcements are often used to strengthen the composite structure. The differences between polymer matrix and ceramic matrix are shown in Figure 2.1 (Campbell, 2010).

While ceramics are used as matrix material, they are generally divided into two as oxides and nonoxides. The best examples of oxide ceramics are alumina (Al_2O_3) and mullite (Al_2O_3-SiO_2) ceramics, which have wide usage. Boron carbide (B4C) and silicon carbide (SiC) are examples of nonxide ceramics.

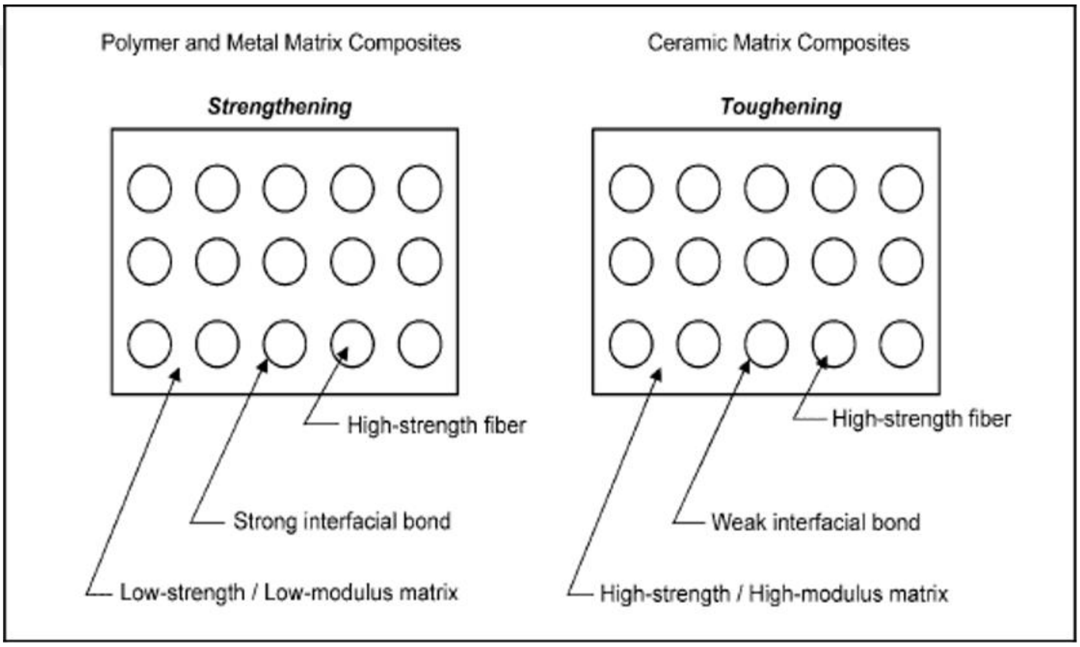

Figure 2.1 Polymer, metal matrix and ceramic composite differences (Campbell, 2010)

2.1.3 Polymer Matrices

Polymer matrix composites are actually plastics (resins) with embedded fibers, and this plastic is called a matrix. Polymer matrix composites have advantages over unreinforced polymers and metals, being light, strong and hard. Allows a variety of design flexibility that can be tailor-made as per the product requirement. If a high performance fiber is reinforced, they can be easily used in the military and aviation industry (Park & Seo, 2011).

A polymer can be defined as a molecule combined with strong covalent bonds and long chains (Mallick, 2007). If these bonds have different chemical properties, they differ from each other as properties. For this reason, polymer matrices are divided into two. These are thermoset and thermoplastic polymers. These are thermoset and thermoplastic polymers.

2.1.3.1 Thermoset and Thermoplastic Polymers

The difference between thermoset and thermoplastic structures can be seen in Figure 2.2.

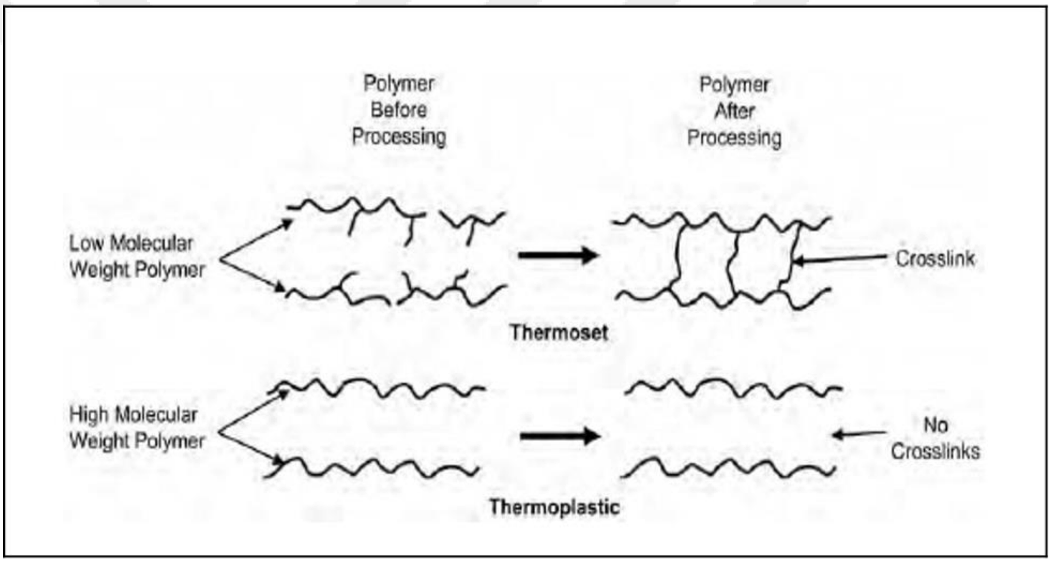

Figure 2.2 Thermoset and thermoplastic structures (Campbell, 2010)

During the late 1990s and 1980s, governments spent millions of dollars to develop thermoplastic, which was their desire to replace the thermoset with thermoplastic material. Despite all these efforts, thermoplastics composites are only used in the production of several commercial and military aircraft. Despite the potential advantages of Thermoplastics, they have not been able to replace thermosets in the aviation industry (Campbell, 2010).

Figure 2.2 shows that the thermoset is cross-linked during hardening to form a hard and solid material. Before hardening, the resin has a low molecular weight structure that melts and flows. However, during the time we leave to cure, the viscosity of the resin starts to increase and at the same time it starts to bond with strong covalent bonds. For these reasons, unless processes are made to increase their toughness, thermoset systems have a fragile structure due to the intensity of the strong cross-links formed (Campbell, 2010).

Unlike thermosets, thermoplastics are high molecular weight resins before being processed. When they enter the process, they melt and flow but do not form a crosslink as seen in Figure 2.2. The main chains are connected by weak bonds, so they can stay together. However, thermoplastic, which are already high molecular weight before the processes, their viscosity increases much higher than the thermosets during the process. Thermoplastic can be reprocessed since no crosslinking occurs during the process (Campbell, 2010).

The reason why thermoplastic can not be used widely in the aviation industry is that they can start to melt as the temperature increases and the polymer structure of the material may become dysfunctional as the temperature increases, since there is no strong covalent connection between them at high temperatures. Figure 2.3 shows the performance comparison of different polymer matrices to each other.

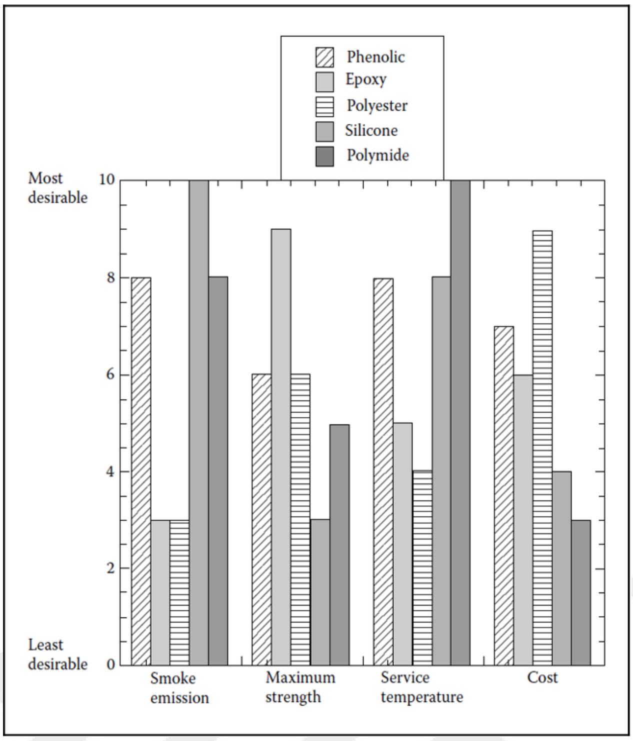

Figure 2.3 Performance comparison of different polymer matrices (Kaw, 2006)

2.2 Reinforcements Materials

Reinforcement elements in composites are responsible for providing high strength and stiffness. The reinforcing elements which are placed in the matrix are stronger than the matrices and we can call these materials fiber. Today, graphite, aramid and glass are the fiber types that are used quite frequently. Today, there are many types of reinforcing elements. These are particle, whiskers and fibers.

We can say that fibers are the most preferred reinforcement element in advanced composite materials since their strength and stiffness properties are very good (Campbell, 2010).

2.2.1 Fibers

Fibers have a rather long axis than particles and whiskers, but they are also generally circular. The fibers have a very strong structure in their long sides, because they are made by drawing method during the manufacturing process (Campbell, 2010).

Fibers generally show higher strength properties than their bulk form. The reason for this is that the defect rate that can occur per unit of length in a material has a lower rate than the defect rate that can occur in the volume of the same material. Since the fibers have a very low volume per unit length, it can be said that it is much stronger than a bulk form with a very large volume per length. Thus, the average and maximum strength will increase as the length increases and the fiber diameter decreases.

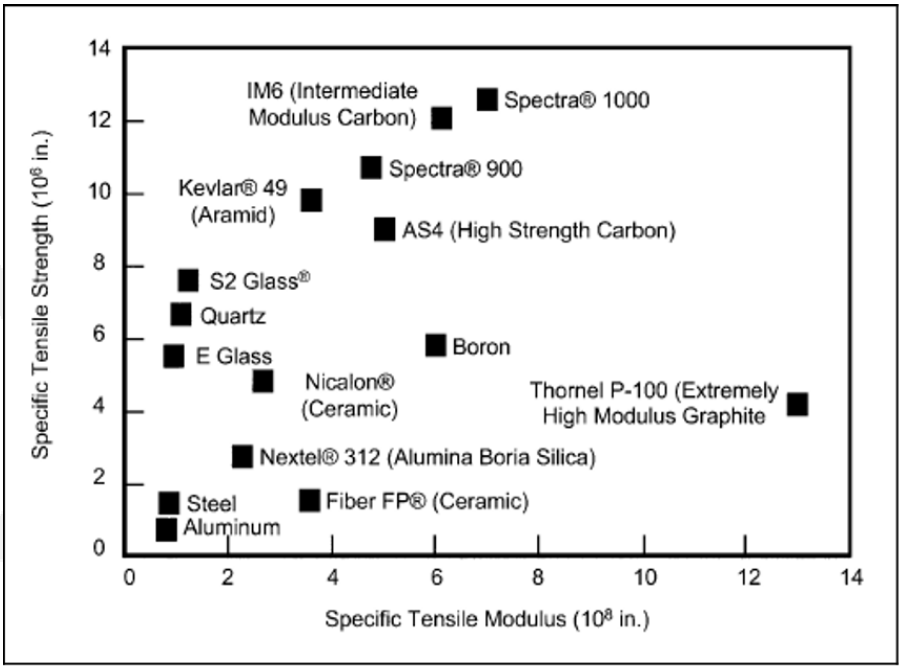

Figure 2.4 Shows the specific tensile strength and modulus graph for commonly used fibers (Campbell, 2010)

2.2.1.1 Glass Fibers

Glass fibers are widely used in commercial applications. Low cost, high impact resistance, high tensile strength and resistance to chemicals are among the prominent features of glass fibers. Despite these superior properties, carbon fibers provide better results in high performance composites (Campbell, 2010).

The disadvantages of glass fibers are that they have high density with low tensile modulus (among the most common commercial fibers), they are highly susceptible to wear during transportation, and therefore their tensile strength decreases, finally, during material processing for cutting tools if they are hard and has low fatigue resistance this situation can cause to overheating and wear.

Although there are many types of glass fibers, the most known and used types are E-glass and S-glass. E-glass is the most widely used material in commercial applications since it has the lowest cost of all reinforcing elements available in the market. S-glass, on the other hand, is a fiber type developed for aircraft and missile parts at the time of its first production, due to the highest tensile strength among all fibers (Mallick, 2007). Figure 2.5 shows the stress-strain curves comparison for high-strength fibers.

Just like the window and container glasses we use, the main ingredient of all glass fibers is silica (SiO_2). Al_2O_3 and B_2O_3 oxides are added to glass fibers to ensure that SiO_2 can be processed by changing the network structure. By keeping the Na_2O_3 and K_2O content of E-glass and S-glass fibers low, corrosion and surface resistance against water is increased. Glass fibers are randomly a three-dimensional network of long silicon, oxygen and other atoms. In this structure, glass fibers provide non-crystalline and equal properties in every direction (Mallick, 2007).

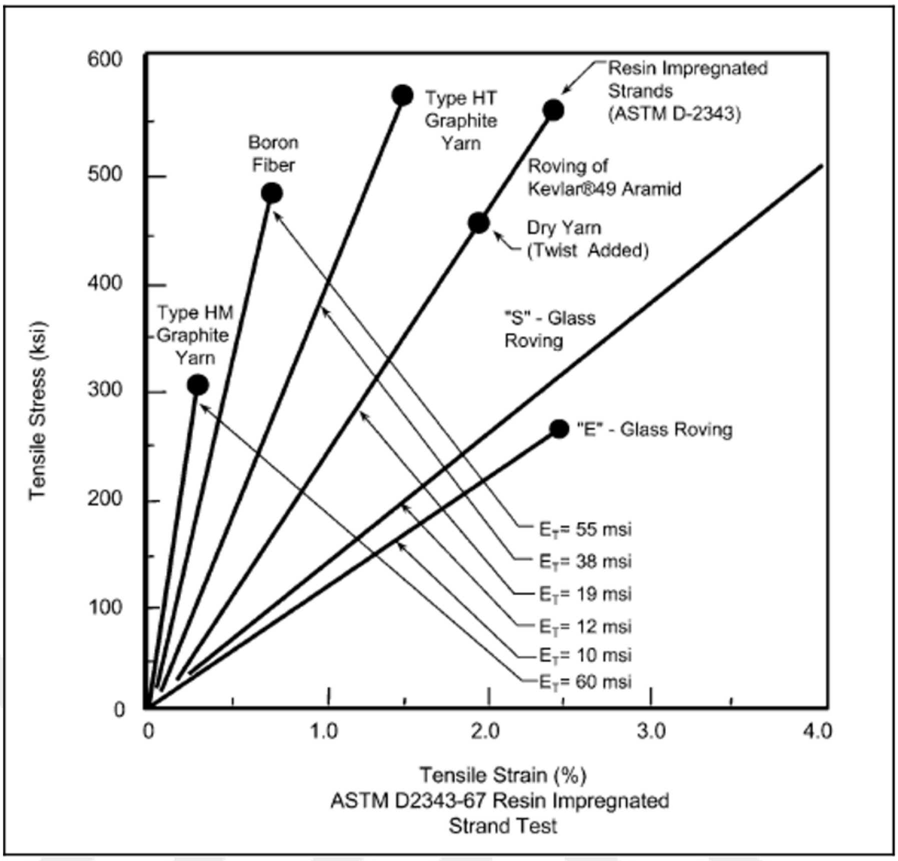

Figure 2.5 Comparison of stress-strain curves for high-strength fibers (Campbell, 2010)

Table 2.1 shows the chemical mixture of E-glass and S-glass.

Table 2.1 E-glass and S-glass chemical compositions (Mallick, 2007)

Type	SiO_2	Al_2O_3	CaO	MgO	B_2O_3	Na_2O_3
E-glass	54.5	14.5	17	4.5	8.5	0.5
S-glass	64	26	-	10	-	-

2.2.1.2 Aramid Fibers

Aramid fibers, which have the highest tensile strength/weight ratio among the existing fibers, are also the lowest density organic fibers. The most popular name on the market is Kevlar 49. Aramid fibers used in the aviation and marine industries are known for their high tensile strength and good properties against impact damage. Just like carbon fibers, complex processing and low pressure resistance are some of the disadvantages of aramid fibers (Mallick, 2007).

Kevlar 49, an aramid fiber, allows it to be used for ballistic protection, as it is an extremely tough material. The ability to absorb energy during fracture is perhaps its most important feature, and its vibration damping coefficients are quite high, as well as having very low thermal conductivity is a disadvantage of Kevlar 49 (Campbell, 2010).

2.2.1.3 Graphite Fibers

The most used fiber type in composite structures is graphite fibers. Resistance to corrosion, having high tensile and compressive strengths and have good properties against fatigue can be listed as their major advantages. Graphite fibers with elastic modules of 345 GPa and containing more than 99 percent carbon are subjected to heat treatments above 1650°C. Graphite fibers also have a three-dimensional array of atoms (Campbell, 2010). Figure 2.6 shows the crystal structure of graphite fibers.

As seen in the figure, carbon atoms are in the form of hexagonal layers in the structure of graphite fibers. They have a very high strength thanks to the structure which formed by covalent bonds with a power of 525 kJ/mol. In this structure, crystallites of different sizes can be directed separately. Since the Graphite is formed by subjected to high heat treatments in the structure, the planes are oriented parallel to the fiber axis with the increase of the temperature in the heat treatment (Campbell, 2010).

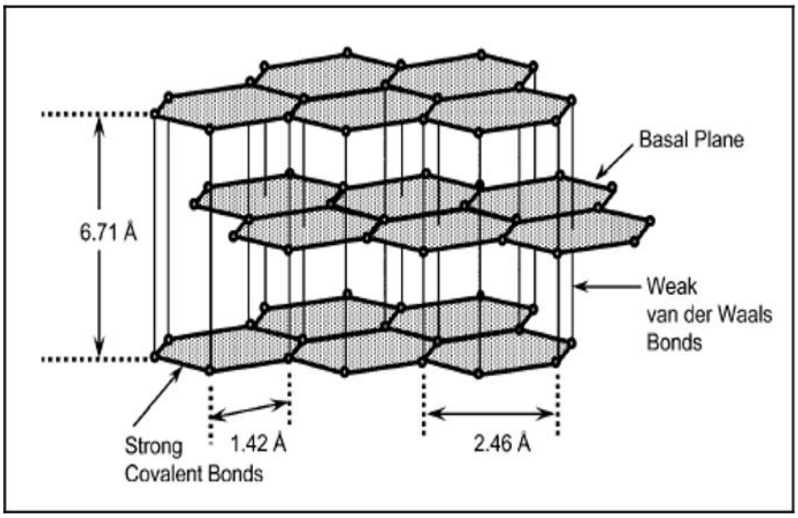

Figure 2.6 Crystal structure of graphite fibers (Campbell, 2010)

2.2.2 Particles and Whiskers

Particles do not have a direction and have a minimal effect on the mechanical properties of materials. They serve as filling material in order to reduce the cost price of the material which desired to create (Campbell, 2010).

Whiskers is very powerful but it creates a disadvantage in terms of use as it is very difficult to distribute homogeneously in the matrix. Compared to fibers, both its diameter and length are smaller (Campbell, 2010).

2.3 Laminated Composites

A single layer of unidirectional or woven fibers in the matrix is called a lamina. Lamina are usually 0.125mm thick. Laying of laminates in a composite pile is called laminate. In laminates, each layer can be laid in various directions and can contain different types of materials. It is very important to know the mechanical properties of a laminate. For example, a suspension system made of laminates such as leaf spring used in cars is constantly subjected to bending and twisting loads. Therefore, when designing this system, the mechanical properties of laminates in stresses and strains should be known. If a composite contains more than one different laminate or fibers, this system is called hybrid composites (Kaw, 2006).

The vast majority of composite materials are not isotropic or homogeneous. The best example is glass/epoxy composite materials. If two different points selected on the glass/epoxy composites are examined, different properties will be seen at both points. This means that the composite is not homogeneous. In addition, the strength in the glass/epoxy composite in the parallel direction to the fibers and the strength in the vertical direction to the fibers are not the same. This means that the properties of glass/epoxy composite are not independent in terms of direction and this makes the glass/epoxy composite material an anisotropic material (Kaw, 2006). Figure 2.7 shows the schematic analysis of laminated composites.

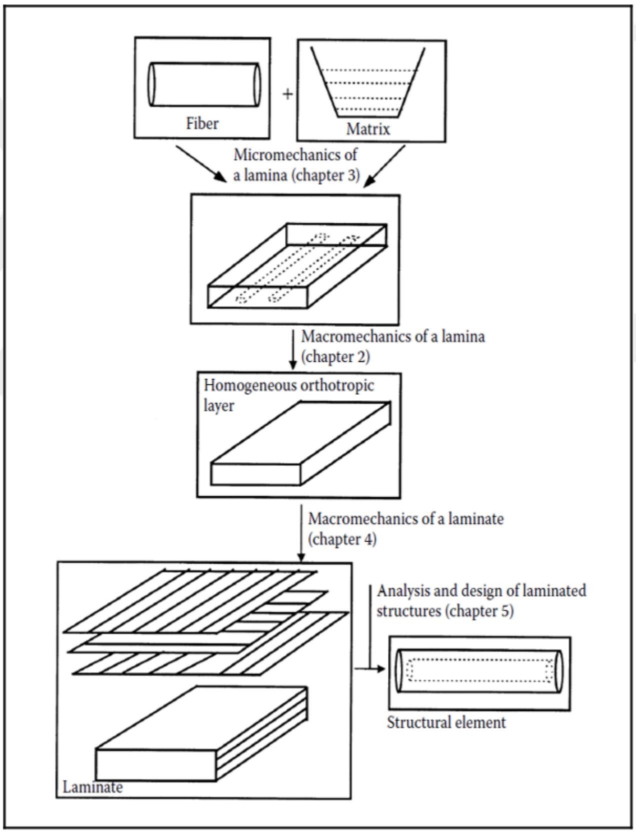

Figure 2.7 Schematic analysis of laminated composites (Kaw, 2006)

CHAPTER THREE
MATERIALS AND METHOD

In this section, the production of S2 glass/epoxy composite material, post-production processes, and the introduction of the devices to be used in the experiments will be included. All the studies and devices used were carried out in Composite Research and Test Laboratory of the Mechanical Engineering Department of Dokuz Eylül University.

3.1 Production of Composite Materials

Composite materials are used in many fields instead of traditional materials. Examples of these are aircraft, space, automotive and marine applications. The main reason for this is that composite materials have high hardness, strength and resistance to temperature and chemical materials. In addition to all these features, they have easy process ability. After these advantages, various methods have been developed for the production of composite materials all over the world. Thus, various production methods have been developed according to the desired requirement and where the material will be used (Goren & Atas, 2008).

Vacuum Assisted Resin Infusion Molding (VARIM) is used today as a very popular composite material production method. In the VARIM method, the resin is drawn under vacuum without being pumped under pressure. Due to its low cost and applicability to large structures, it is becoming an increasingly important composite material production technology (Goren & Atas, 2008). Figure 3.1 shows the schematic representation of the VARIM process.

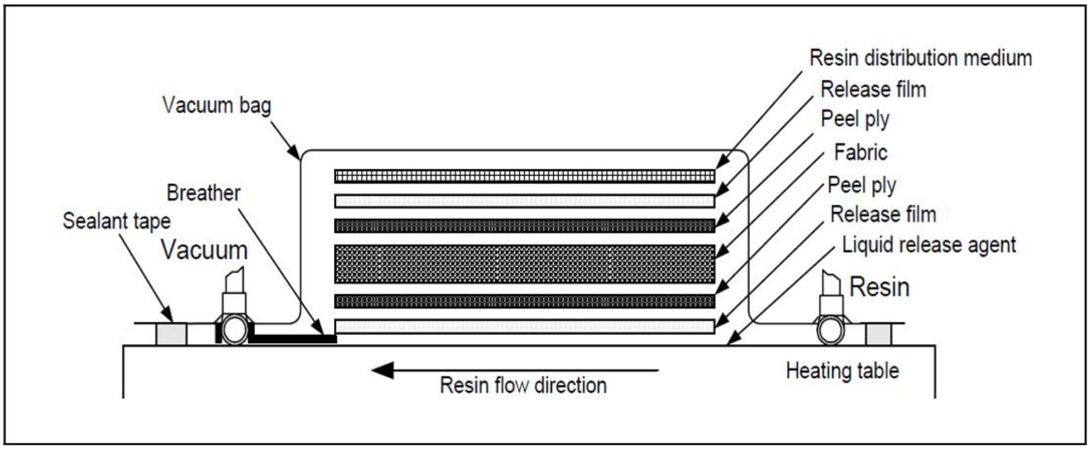

Figure 3.1 Shows the schematic representation of the VARIM process (Goren & Atas, 2008)

The production steps with the VARIM method can be explained as follows: The edges of the mold release agent to be used are covered with adhesive sealant. Then the top of the counter/workbench is covered with the same mold release agent. Thanks to this process, epoxy drawn with a vacuum is prevented from sticking on the workbench. In the second step, S2 glass fabrics are placed on the workbench which covered by mold release agent. Then, peel ply is placed on S2 glass fabric, the task of this fabric is to prevent S2 glass fabric from sticking to the vacuum bag with the resin dispenser. In the fourth stage, resin dispersant is placed on the peel ply and the resin is well distributed on the composite material. In the fifth and last step, spiral pipes are placed on both sides and covered with a vacuum bag. After these processes, the vacuum is opened and the air inside is drawn. In order to check that there is an air leak, one should wait for a while after the air is drawn. If there is no leakage after the control, the mixture of epoxy and hardener is prepared so that the hardener/epoxy ratio is 1/3. After giving the resin, it is necessary to wait for curing. The curing time in this study is 30 minutes at 50°C for pre-curing and then 8 hours at 80°C for the rest of the process. Figure 3.2 shows the composite production system. Here, the workbench is heated using electrical heating residences. Thanks to the thermocouples on it, the temperature is kept under control.

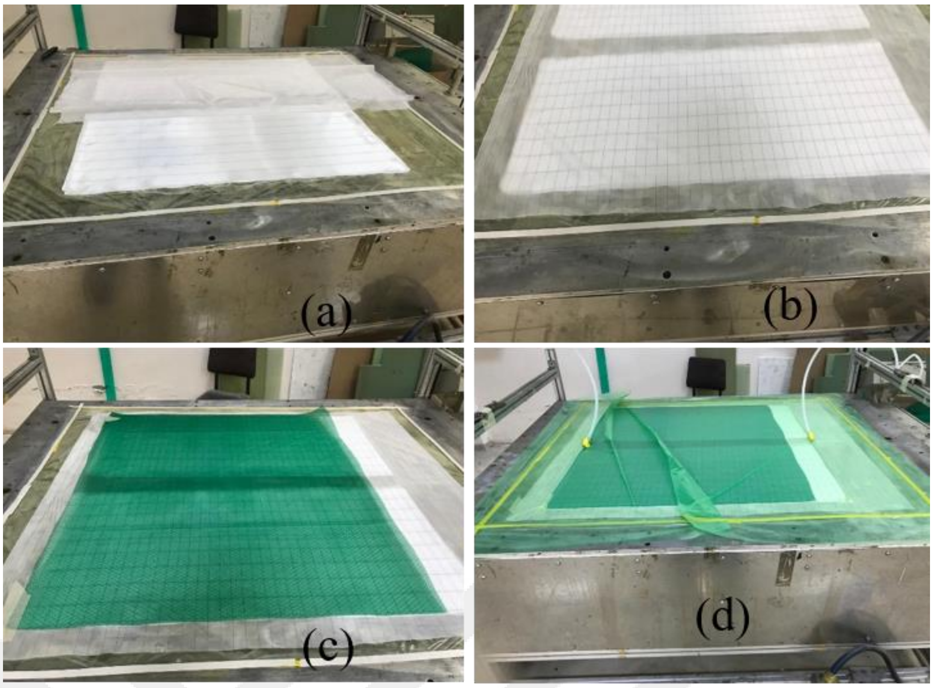

Figure 3.2 a) S2 glass fabrics on mold release agent on, b) peel ply is placed on S2 glass fabrics, c) resin dispersant placed on the peel ply, d) whole system covered with vacuum bag (Personal archive, 2020)

S2 glass fabric/epoxy composite material was cut by the water saw in order to obtain the desired size of 100mmx150mm samples. Figure 3.3 shows the water saw.

Figure 3.3 The water saw for cutting sample (Personal archive, 2020)

3.2 Impact Test

CEAST Fractovis Plus was used as an impact device. The impact energy capacity of this device, which is used for low-velocity impact testing, is 1800J. In this device, which operates with the principle of weight reduction, if a bounce condition occurs on the sample, the anti-rebound system is activated and prevents rebound. In the impact device, impact tests are carried out in a closed air-conditioning section. Thus, impact tests can be performed at temperatures between -100°C and 150°C. Since the tests to be performed in this study will be applied under room temperature, liquid nitrogen is used for the cooling process. Thanks to the liquid nitrogen filled in the tank, impact tests can be performed at the desired low temperature values. Thanks to the redundant sensors, the impact device can reliably reach a maximum speed of 24m/s. The hemi-spherical tip used in impact experiments has a diameter of 12.7mm. Thanks to the impact device (DAS), data such as contact force-time, velocity-time, displacement-time, energy-time and energy-displacement graphics of impactor can be obtained. Figure 3.4 shows CEAST Fractovis Plus impact test machine, test specimen and liquid nitrogen tank.

Figure 3.4 a) CEAST Fractovis Plus impact test machine, b) test specimen, c) liquid nitrogen tank (Personal archive, 2020)

3.3 Compression-After Impact (CAI) Test

CAI tests are performed after impact test on S2 glass fabric/epoxy samples. The samples in the tests are prepared for use in the Boeing CAI test fixture (ASTM D 7137). Figure 3.5 shows the CAI test application. As shown in Figure 3.5b, the sample is locked with top and bottom edges. There are lateral supports to prevent twinning.

For the Shimadzu AG-X testing machine with a load capacity of 100 kN, the compression speed used during the test is considered as 1 mm / min. In the tests performed according to ASTM D 7137 standards, the sample dimensions must be 150mm long and 100mm wide. CAI strength is obtained by using equation (3.1).

$$\sigma_c = \frac{F}{b.t} \tag{3.1}$$

Where, σ_c is CAI strength, F is the compression force in failure, b is the sample width and t is the sample thickness.

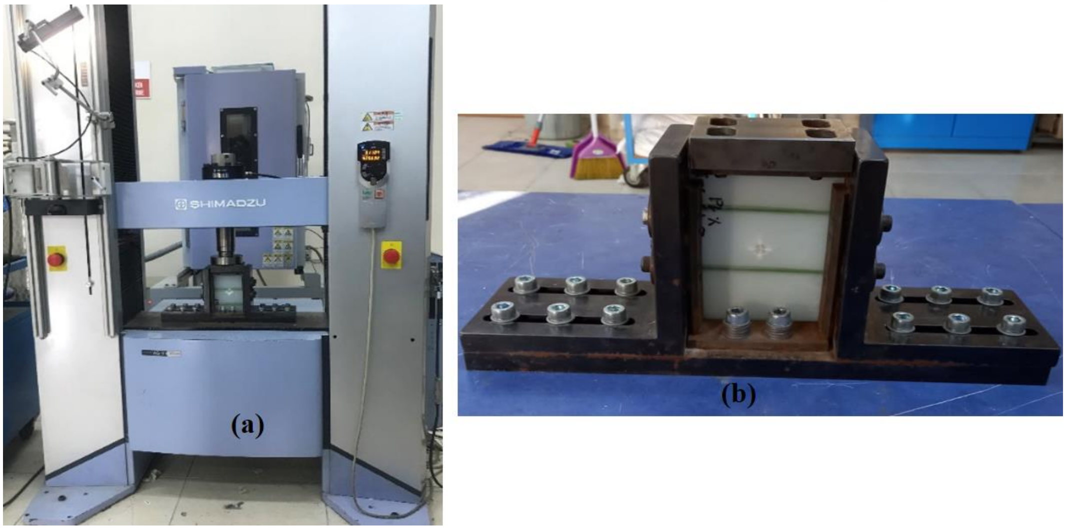

Figure 3.5 a) Shimadzu AG-X tension/compression testing machine with compression-after impact (CAI) apparatus, b) CAI test apparatus (Personal archive, 2020)

CHAPTER FOUR
RESULTS AND DISCUSSION

The properties sought in composite materials vary according to where and under what conditions the material will be used. In this study, S2 glass/epoxy composite material was chosen as the composite material. The low velocity impact behavior of composite materials has been discussed from different aspects, and the material has been examined and investigated by CAI tests.

Within the scope of this study, composite materials were produced in two different thicknesses of 2.72mm and 3.02mm. Then samples were prepared in 100mmx150mm dimensions. After that, low velocity impact tests were applied to these samples. The samples were tested at three different impact energies (30J, 40J and 50J) and at three different temperatures (20°C, -25°C and -50°C). After the low velocity impact tests were applied, the samples were examined by force-time and energy-time graphs.

CAI test was applied to samples after low velocity impact tests. These tests were applied at 20°C. As stated above, since the samples contain two different thicknesses, three different energies and three different temperatures, each experimental group was evaluated separately in CAI tests.

Since the samples used in this study depend on different composite thickness, energy levels, temperature and test type, this study consists of three main parts. These working steps are as follows:

- Impact Results
- CAI Results

4.1 Impact Results

In this study for the further investigation of impact results, absorbed energy, elastic energy, maximum contact force, maximum displacement and contact time values of specimens were calculated. Table 4.1 shows the calculated average values of the samples subjected to the low velocity impact test at 20°C, -25°C and -50°C temperatures and 30J, 40J and 50 impact energies, respectively. When Table 4.1 is examined, it is seen that the maximum displacement decreases as the temperature decreases in the experimental groups at the same impact energy for the samples with 2.72mm and 3.02mm thicknesses.

Table 4.1 Low velocity impact test results for different temperatures and energies

Temperature	Thickness [mm]	Impact Energy [J]	Absorbed Energy [J]	Elastic Energy [J]	Maximum Contact Force [N]	Maximum Displacement [mm]	Contact Time [ms]
20°C	2.72	30	10.64	19.36	5430	15.45	11.76
		40	18.52	21.48	5448	19.17	16.79
		50	48.78	1,22	5204	14.92	8.16
	3.02	30	8.72	21.28	6398	14.21	8.65
		40	14.71	25.29	6721	17.13	10.12
		50	24.19	25.81	6801	20.14	11.77
-25°C	2.72	30	7.73	22.27	5771	15.33	11.58
		40	23.35	16.65	6584	18.74	14.56
		50	46.03	3.97	5984	12.9	6.30
	3.02	30	1.22	28.78	7922	13.61	8.61
		40	6.54	33.35	8052	16.59	10.12
		50	17.33	32.67	7878	19.89	11.76
-50°C	2.72	30	4.33	25.67	6733	14.69	10.98
		40	21.08	18.92	6816	17.75	11.32
		50	47.99	2.01	7307	12.6	7.64
	3.02	30	2.09	27.91	8603	13.43	7.97
		40	7.32	32.68	8474	16.10	9.24
		50	16.7	33.3	8253	19.36	11.83

4.1.1 Contact Force

In this part of the experiment, the specimens with two different thickness and 100mmx150mm dimensions were subjected to the impact tests at different temperatures and energies by at least five test repetitions. In Figure 4.1, the force-time graphics of composite material with thickness of 3.02mm subjected to impact loading at 20°C and 30J have been presented. As it can be seen, the experimental results are very similar each other. Here, during the selection of graphics, the average values of these and other test group samples are taken.

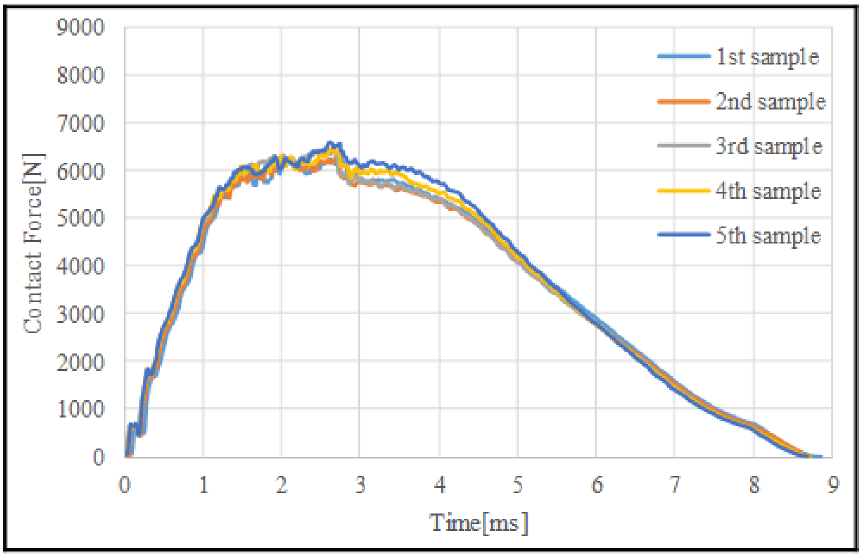

Figure 4.1 Force-time graphics of at samples with 3.02mm thickness for 20°C and 30J energy

Figure 4.2 shows contact force-time diagrams according to the impact energy for different temperatures and sample thicknesses.

When the graphics are examined, it is seen that the initial monotonic increase by impact event corresponds to the elastic bending of the composite material. This increase continues in the form of small oscillations up to a certain load value, for example until a sharp decrease due to the onset of damage due to impact energy and temperature. The small oscillations here are basically just the breakdown of the matrix. The maximum load is reached after the matrix is completely broken. Until the maximum load is reached, the significant drop in load is due to the spread of damage to the composite material. Breaking of the fibers takes place at this time. The part after the breakage of these fibers consists of residual stresses and impactor friction against the composite plate (Boumbia et al., 2017).

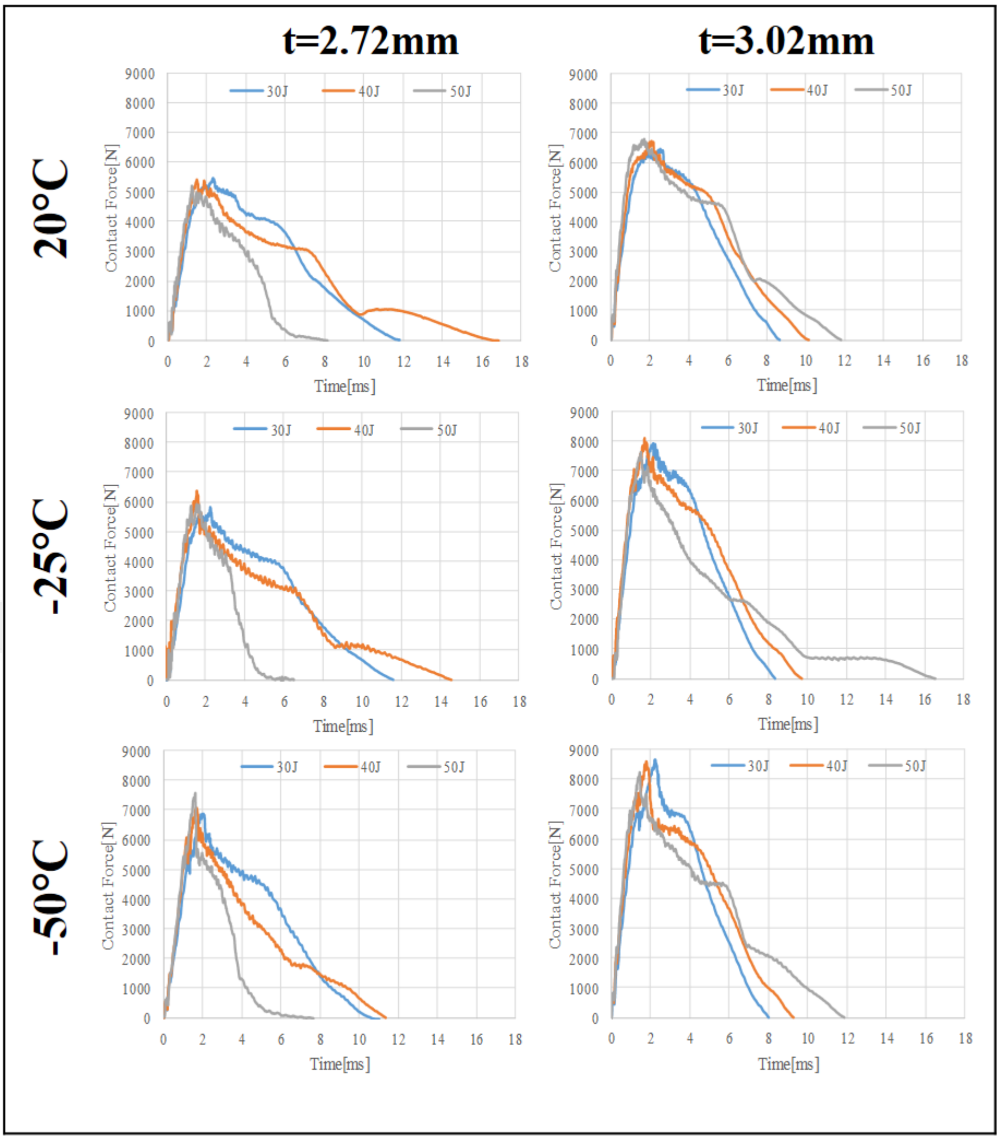

Figure 4.2 Contact force-time graphs according to the impact energy for different temperatures and thicknesses

When the graphs of the sample with 2.72mm thickness is examined, it is seen that the impact test at 50J energy has the shortest duration. The reason for this can be that the composite material undergoes penetration for all three temperatures. It is seen that 40J energy has a higher duration at all three temperatures compared to 30J energy. The reason for this is that the impactor does not penetrate at energy values of 30J and 40J, and when the impactor hits the material, it rebounds, in other words, the impactor hits the material and rises back and falls again. In the rebound movement, the duration of the experiment is prolonged since the impactor that comes with high energy value will bounce up more than the material.

When the graphs of the sample with 3.02 mm thickness is examined, it is seen that impact tests at 30J energy have the shortest duration, while 50J energy has the highest duration. The reason for this is that the material does not undergo penetration in the 30J, 40J and 50J impact energies, and therefore the greatest rebound movement occurred at the highest energy level, 50J.

Figure 4.3 gives contact force-time graphs according to the temperature for different impact energy and thicknesses.

When Figure 4.3 is examined, the maximum contact force increases as the temperature decreases in all 30J, 40J and 50J energy values of the samples with 2.72 mm and 3.02 mm thicknesses because of the residual stresses caused by decrease in temperature.

When the graphs are examined for 2.72 mm thickness, the maximum contact force increases by 12.13% when decreasing the temperature from 20°C to -25°C, the maximum contact force increases by 13.24% when the temperature was decreased from -25°C to -50°C.

When the graphs of sample with 3.02mm thickness are examined, the maximum contact force increases by 16.48% when the temperature is reduced from 20°C to -25°C, while the maximum contact force increases by 5.83% when the temperature falls from -25°C to -50°C.

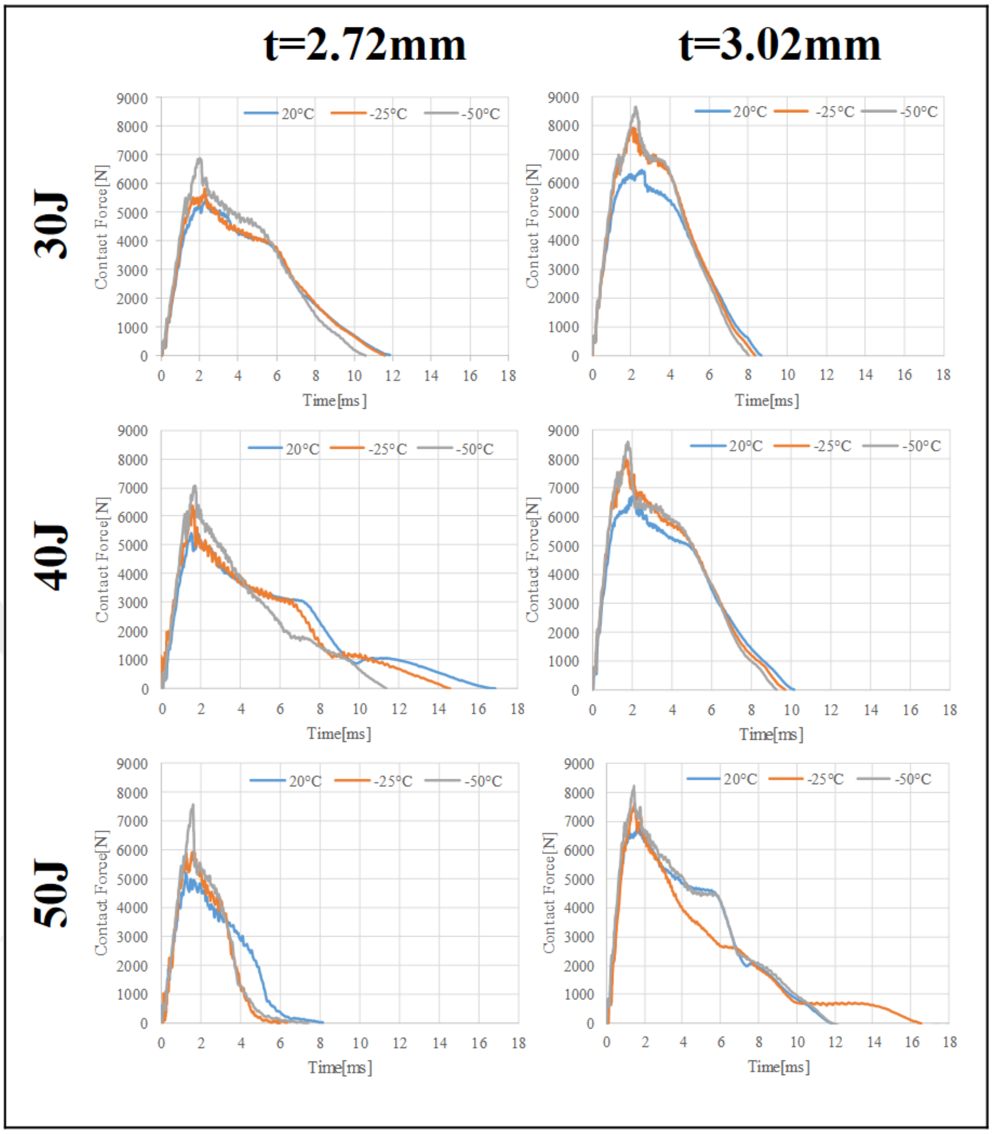

Figure 4.3 Contact force-time graphs according to the temperature for different impact energy and thicknesses

Figure 4.4 shows contact force-time graphs according to the thickness for different impact energy and temperatures.

When Figure 4.4 is examined, it is seen that the maximum contact force increases in all graphic types with the increase of thickness. On the contrary, it is seen that the impact duration decreases as the thickness increases. From here, it can be observed that the increase in the thickness restricts the rebound movement of the impactor. The reason why the thin sample at 50J impact energy has a shorter impact duration is that the test sample is penetrated at this energy.

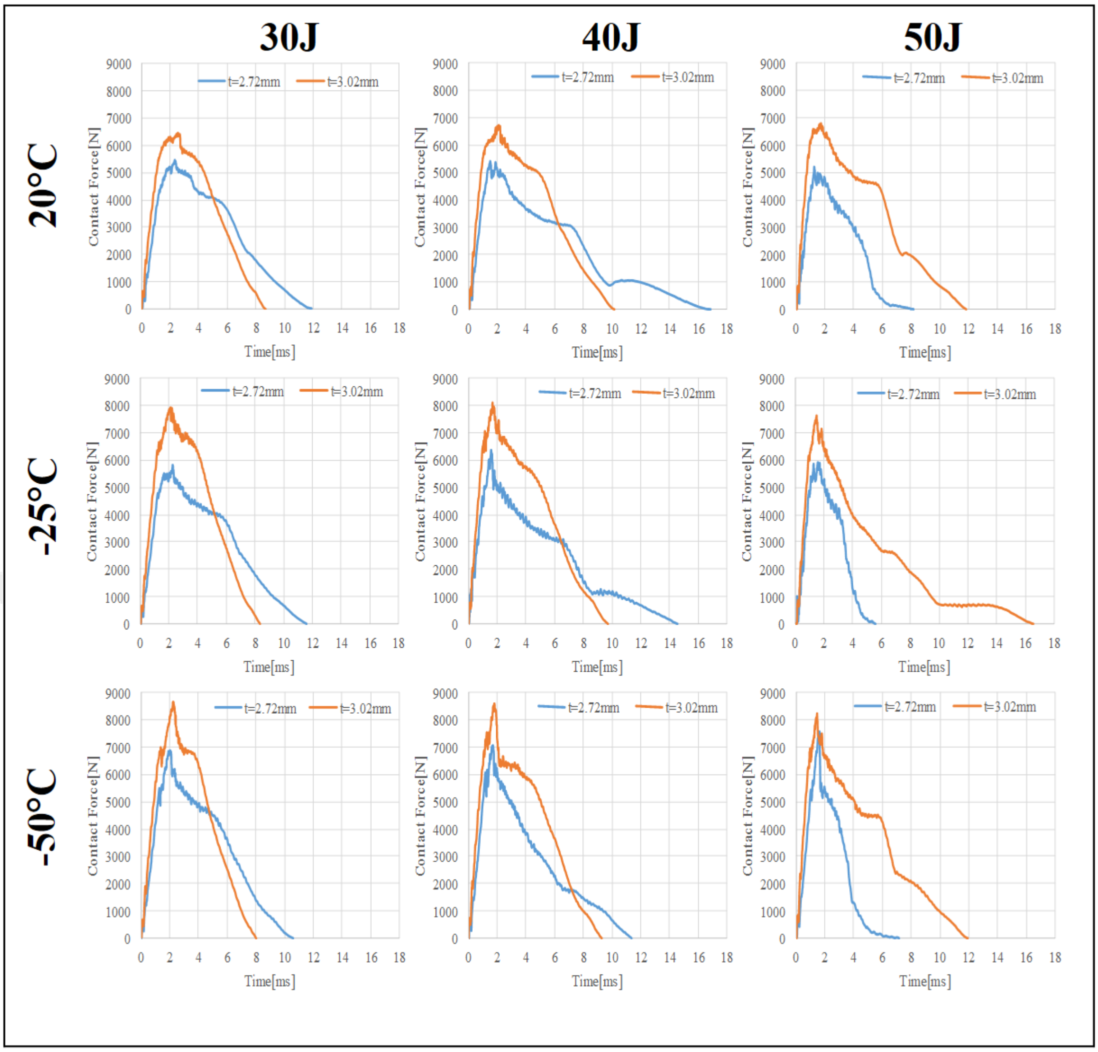

Figure 4.4 Contact force-time graphs according to the thickness for different impact energy and temperatures

Figure 4.5 illustrates maximum contact force change due to energy change of composites with a) 2.72mm and b) 3.02mm thicknesses for different temperatures.

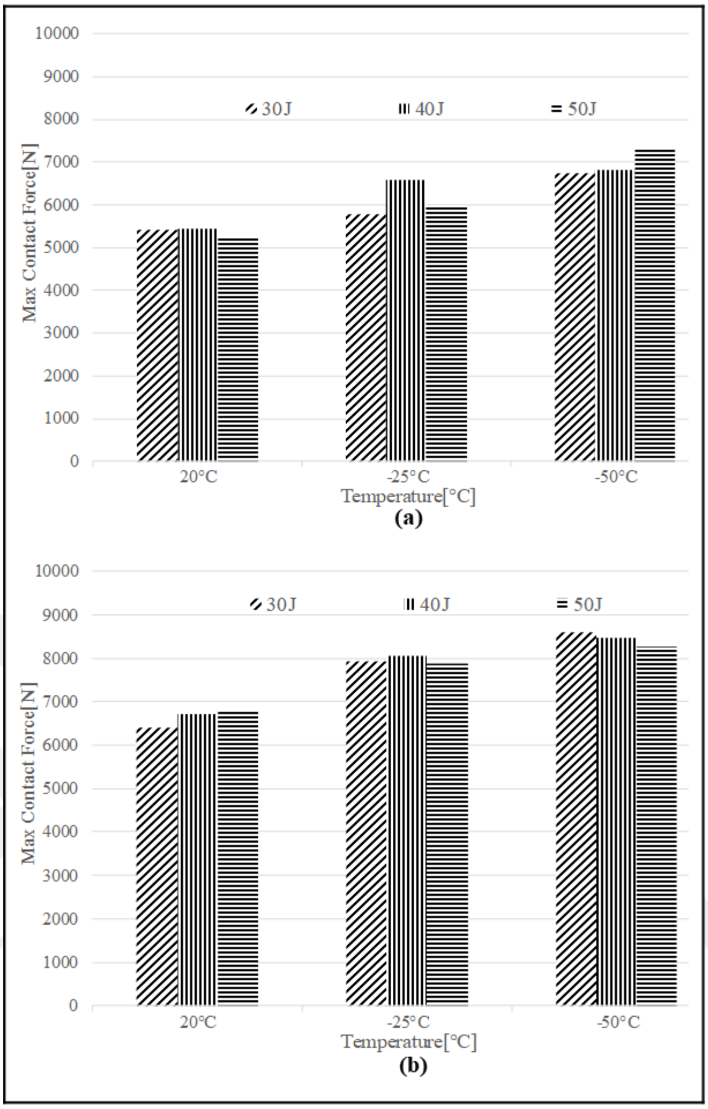

Figure 4.5 Maximum contact force change due to energy change of composites with a) 2.72mm and b) 3.02mm thicknesses in low velocity impact test

When the graphs in Figure 4.5 are examined, it is seen that the highest maximum contact force in composite materials with 2.72mm thickness occurres at -50°C and 50J, and its value is 7307N. In the same thickness, the lowest maximum contact force occurres at 20°C and 50J and its value is 5204N.

When the composite materials with 3.02mm thickness were examined, it is seen that the lowest maximum contact force occurres at 20°C and 30J and it has the value of 6398N. In the same experimental group with a thickness of 3.02mm, it was observed that the highest maximum contact force occurres at -50°C and 30J and it has the value of 8603N.

Based on these results, it has been observed that the increase in impact energy gives different force distribution at each temperature value in composite materials with 2.72mm thickness. Likewise, in composite materials with 3.02mm thickness, the maximum contact force varies depending on the temperature as the energy increases.

As the energy increases, the maximum contact force increases. This is because when the impactor hits the composite material, the impact may result in loss of contact between the impactor and the material. As soon as the impactor hits the material, the S2 glass/epoxy layers in the back region of the composite material may suddenly be detached, resulting in loss of contact with the impactor on the material surface. When the impactor passes the gap caused by the separation of the layers, an increase in the load occurs again (Boumbia et al., 2017).

In this section, the effect of temperature change is examined. Figure 4.6 shows the maximum contact force values obtained by taking the average of the results obtained from each experiment group of the experiments.

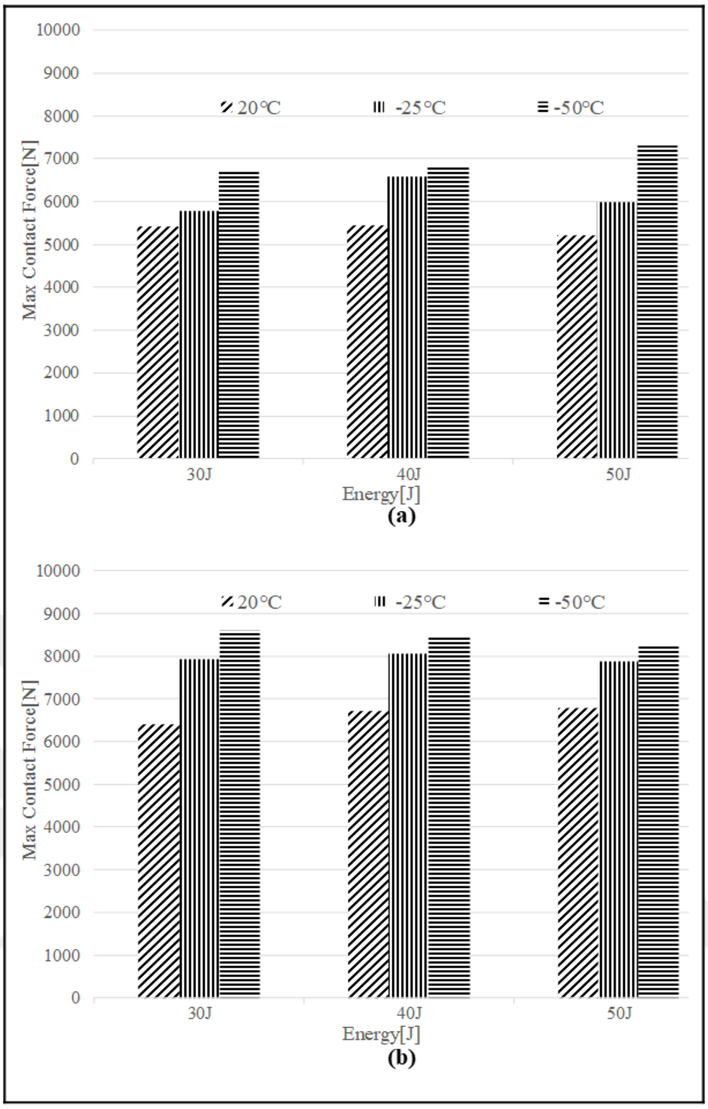

Figure 4.6 Maximum contact force change due to temperature change of composites with a) 2.72mm and b) 3.02mm thicknesses

When the graphs in Figure 4.6 were examined, it was observed that the maximum contact force increases as the temperature decreases in each experimental group. The reason for this is that S2 glass and epoxy material have different thermal expansion coefficients. When these two materials with different thermal expansion coefficients start to cool, the material with a higher thermal expansion coefficient has a more tendency to shorten, resulting in compressive residual stresses between the layers of the two materials. Due to this situation, the rigidity of the material will also increase. In this compressive residual stress, when the impactor hits the sample with a certain energy, it must be reset first. This compressive stress continues to increase up to maximum contact force when residual stresses are reset. As a result, as the temperature drops, the maximum contact force increses.

When the graphs are examined, the maximum contact force value of the sample with 2.72mm thickness is 7307N at -50°C and 50J energy. The lowest value of the contact force was obtained as 5204N at 20°C and 50J energy.

In the graph, the maximum contact force value for samples with 3.02mm thickness is 8603N at -50°C and 30J energy. The lowest force value is 6398N at 20°C and 30J.

In order to see the effect of sample thicknesses on the average maximum contact force in low velocity impact tests, the average values for each test group were plotted to show the thickness effect. In this part of the thesis, the effect of the thickness is examined, and the values of the average results are shown in Figure 4.7.

When Figure 4.7 is examined, it is seen that increasing the thickness of the samples increases the maximum contact force in all test groups. When the graphs in the figure are examined, the highest maximum contact force is at -50°C and 30J for sample with 3.02mm thickness and its value is 8603N. When all experimental groups were examined, it is seen that increasing thickness increases the maximum contact force by 20.06%.

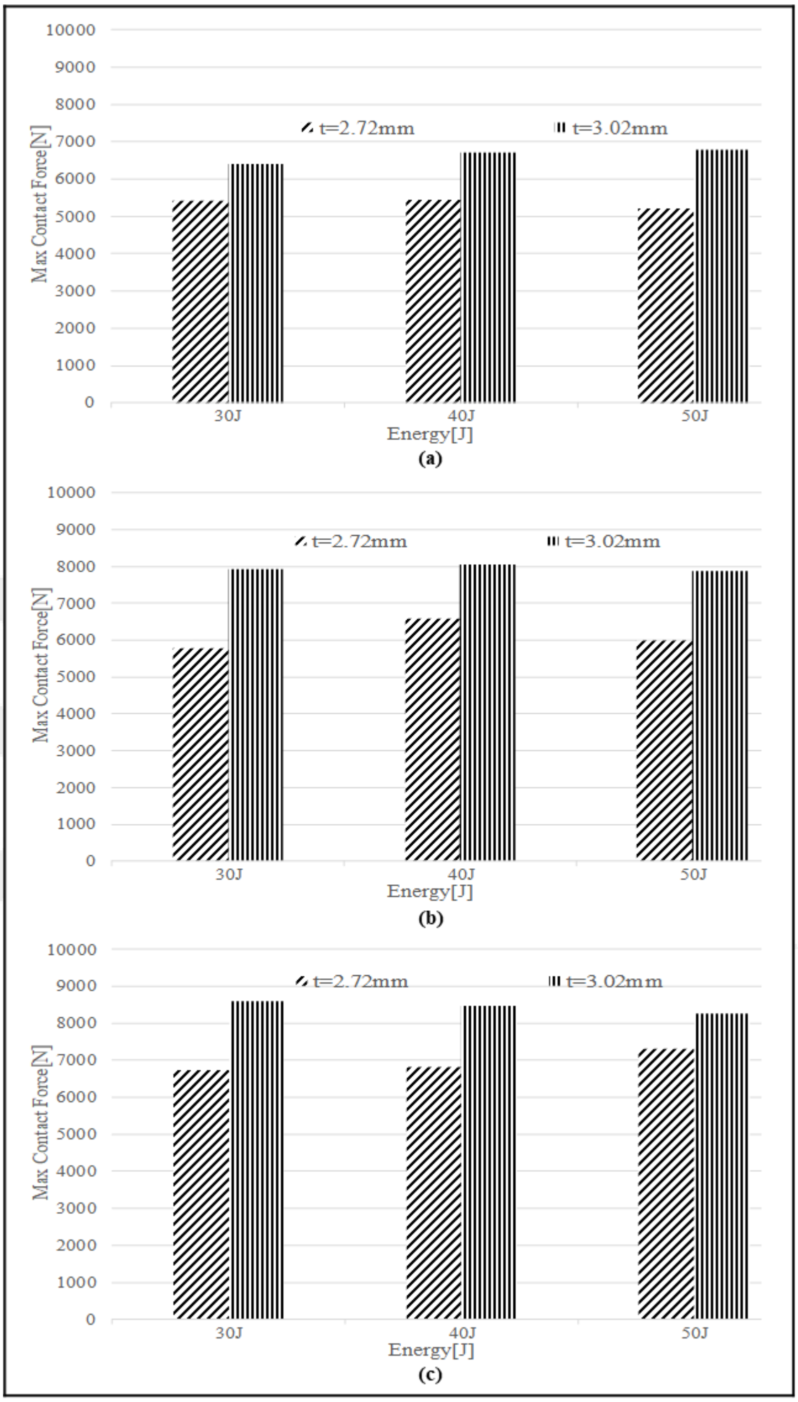

Figure 4.7 Maximum contact force change due to thickness change of composites at a) 20°C, b) -25°C and c) -50°C temperatures

4.1.2 Absorbed Energy

Energy-time graphics provide information about how much energy the material absorbs. The peak energy value in energy-time graphs gives us the impact energy.

Absorbed energy is given by the horizontal part of the energy-time curve after the peak energy. Elastic energy indicates the difference between impact energy and absorbed energy (Boumbia et al., 2017).

Figure 4.8 shows defination of impact energy, absorbed energy and elastic energy on energy-time graph of impact test.

.

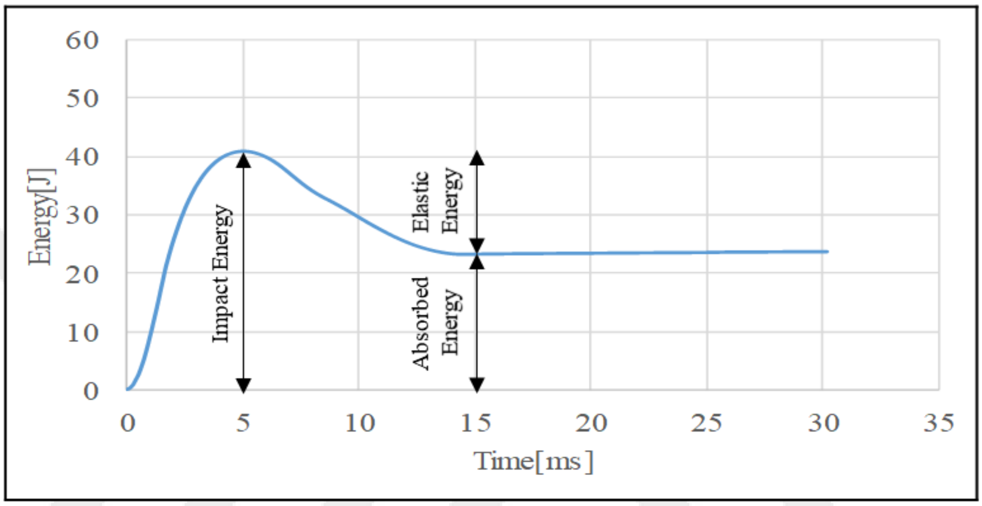

Figure 4.8 Definition of impact energy, absorbed energy and elastic energy on energy-time graph

Figure 4.9 shows the energy-time changes of materials based on energy.

When Figure 4.9 is examined, it is seen that samples with 2.72mm thickness undergo penetration at 50J energy values. At all three temperature values, almost all of the 50J impact energy was absorbed and the energy value of 50J could not be reached. While the absorbed energies are almost equal at 40J impact energy value at all three temperatures, the absorbed energy at 30J impact energy value decreases as the temperature decreases.

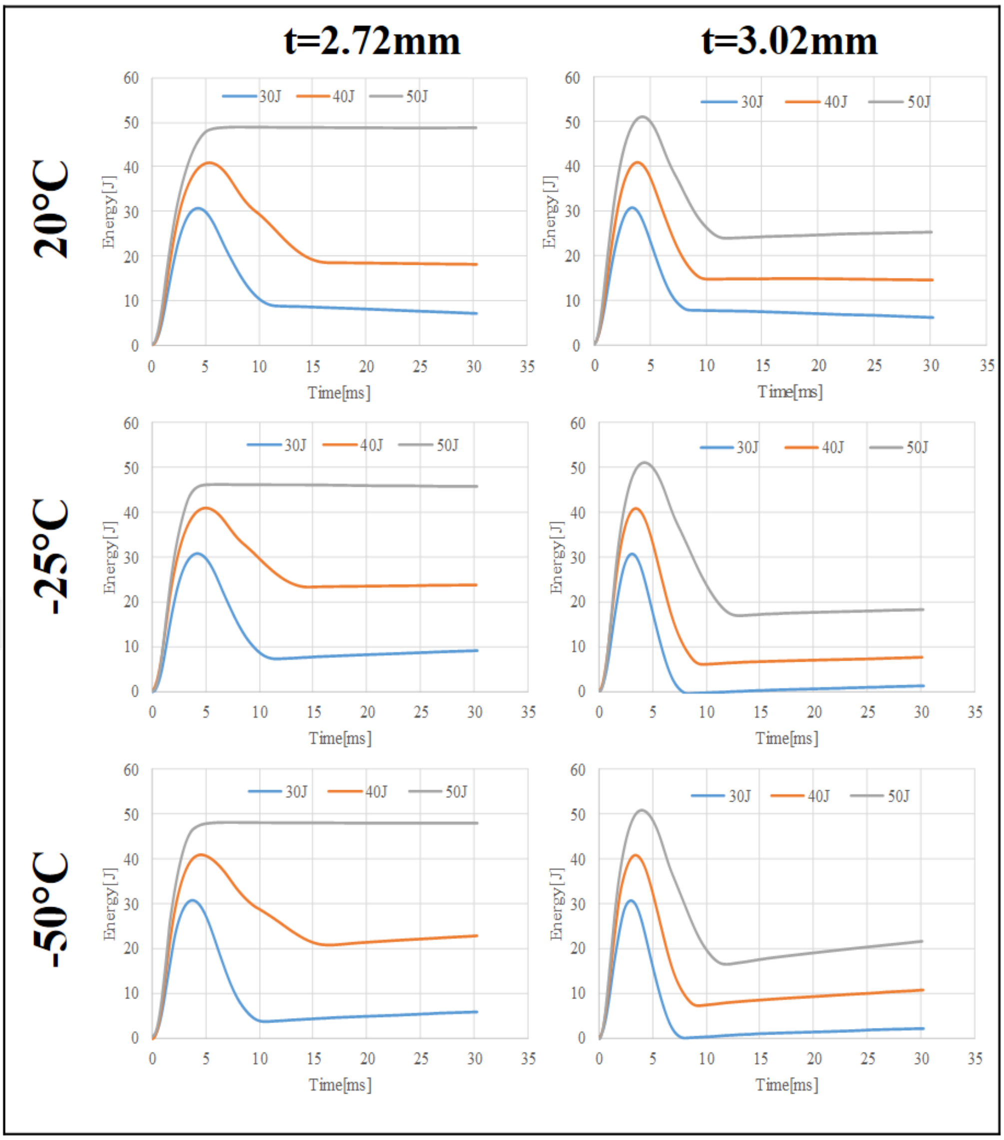

Figure 4.9 Energy-time graphs depending on energy change

In thicker samples with 3.02mm thickness, almost all of the energy remained as elastic energy at 30J impact energy value at both temperatures below 20°C. At 40J and 50J impact energy, the absorbed energy decreases from 20°C to -25°C, while at -50°C the absorbed energy amount remained almost the same as at -25°C.

Figure 4.10 shows the energy-time changes depending on the temperature.

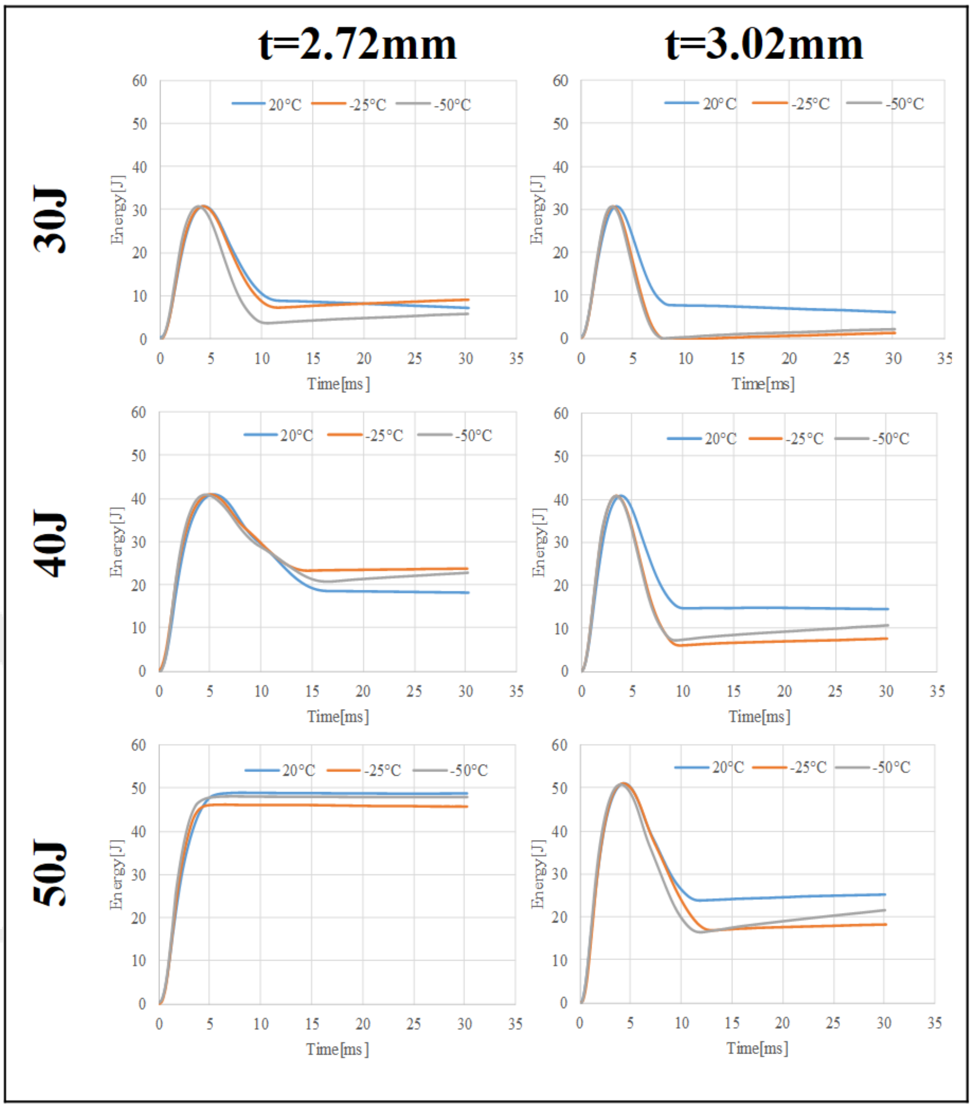

Figure 4.10 Energy-time graphs due to temperature change

When the graphs in Figure 4.10 are examined, for 30J, the absorbed energy decreases due to drop in the temperature in the samples with 2.72mm thickness and the elastic energy increases. The absorbed energy at 40J impact energy is the highest at -25°C, followed by -50°C and 20°C, respectively. For 50J, this impact energy could not be reached since all of the samples were pierced at all three temperatures. When the graphs are examined for samples with 3.02mm thickness at 30J impact energy, absorbed energy decrease at both -25°C and -50°C when the temperature falling below 20°C for 30J. In the impact energies of 40J and 50J, the drop in temperature from 20°C to -25°C and -50°C caused decrease in absorbed energy and increase in elastic energy.

Figure 4.11 shows the energy-time changes depending on the thickness of the materials graphically. When Figure 4.11 is examined, it is seen that the energy absorbed decreases with increasing thickness and elastic energy is more. In all 50J impact tests, it is seen that samples with 2.72mm thickness have undergone penetration.

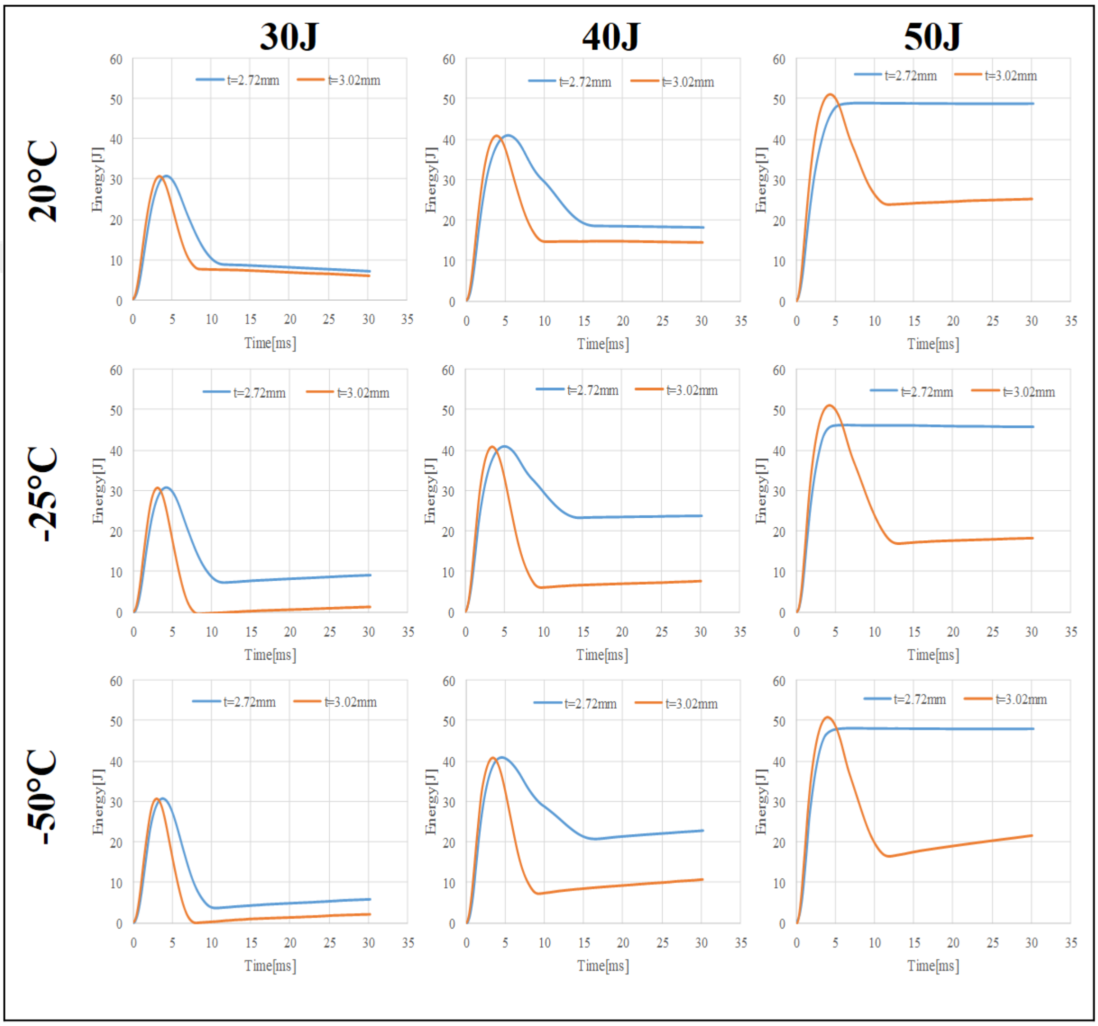

Figure 4.11 Energy-time graphs depending on the thickness of composite materials for different impact energy and temperature

4.1.3 Impact Damage

In this section, damages on the specimen after low velocity impact tests were examined by visual inspection. For this reason, in Figure 4.12, Figure 4.13 and Figure 4.14, the impact tests performed at 30J, 40J and 50J energy values at 20°C, -25°C and

-50°C, respectively, at two different thicknesses, 2.72mm and 3.02mm. The damage to the two impact surfaces and back faces were examined.

The investigation was initiated with samples with 2.72mm thickness. It is observed that the indentation depth decreases as the temperature decreases, especially in the impact tests made at 40J and 50J energies in samples of this thickness. If this situation is examined better, the indentation depth on the impact surface and the back surface in the impact tests performed at 40J at 20°C is noticeably reduced at -25°C. Likewise, when decreasing from -25°C to -50°C, the indentation depth on the back surface decreases. This situation continues in 50J impact damage as well in samples with 2.72mm thickness. The decrease in indentation depth can be explained by the stiffness of the samples increasing as the temperature decreases. It was observed that samples were pierced at all three temperature values at 50J impact energy. But here, too, it is seen that the indentation depth at the puncture site decreases as the temperature decreases. In the impact tests with 30J energy, it was observed that there was not a noticeable difference as the temperature decreases due to the low energy, but it can be said that the impact surface received less indentation depth.

If we continue the analysis with samples 3.02mm thickness, as stated above, when the temperature drops from 20°C to -25°C at 30J impact energy, it is seen that the indentation depth decreases considerably. It is seen that there is no noticeable difference in this energy value when it is reduced from -25°C to -50°C. In the impact tests performed at 40J energy, it is seen that the puncture damage occurred on the back surface of the impact decreases as the temperature decreases, while there is no visible difference at all three different temperatures on the impact surface. Similar to test with 40J energy, in tests with 50J energy there is not a variation on impact surface with respect to temperature, while with the decrease in the temperature, in the back side of the sample the indentation depth is reduced. Thus, it can be said that with the decrease in the temperature and increase in stiffness the indentation depth would decrease. With the increase in the impact energy, the damaged area of all samples are also increased for all three given temperature values.

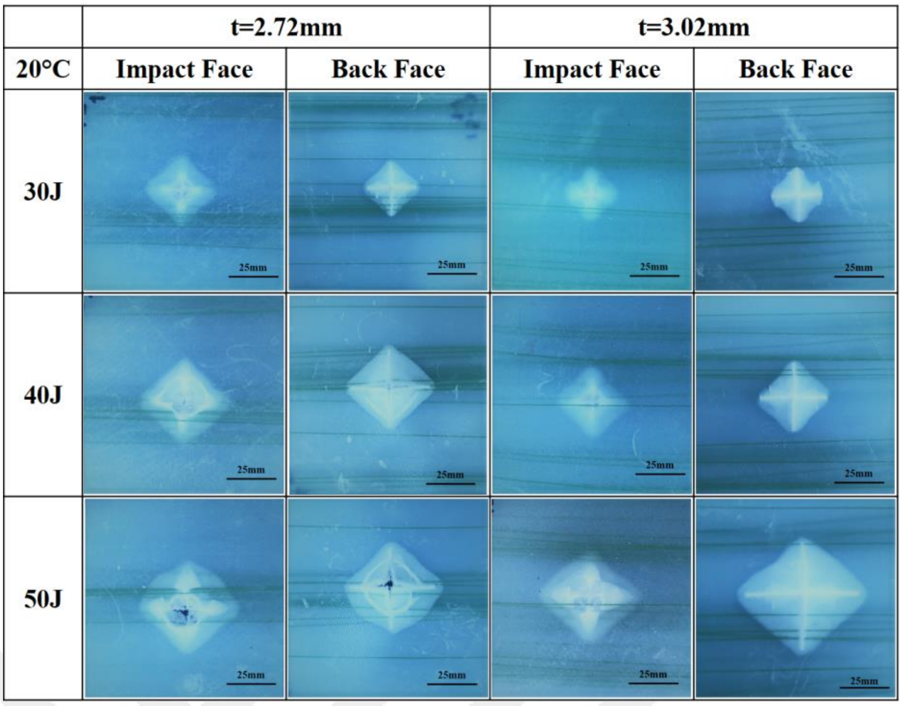

Figure 4.12 Impact damages types of S2/glass epoxy samples with 2.72mm and 3.02mm thicknesses at different impact energies at 20°C

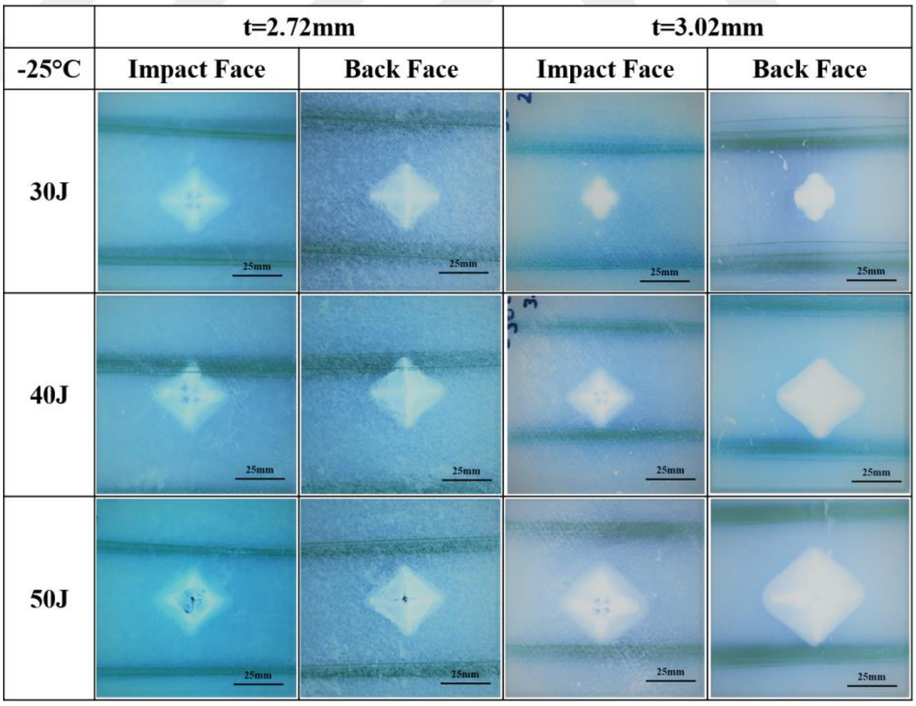

Figure 4.13 Impact damage types of S2/glass epoxy samples with 2.72mm and 3.02mm thicknesses at -25°C at different impact energies

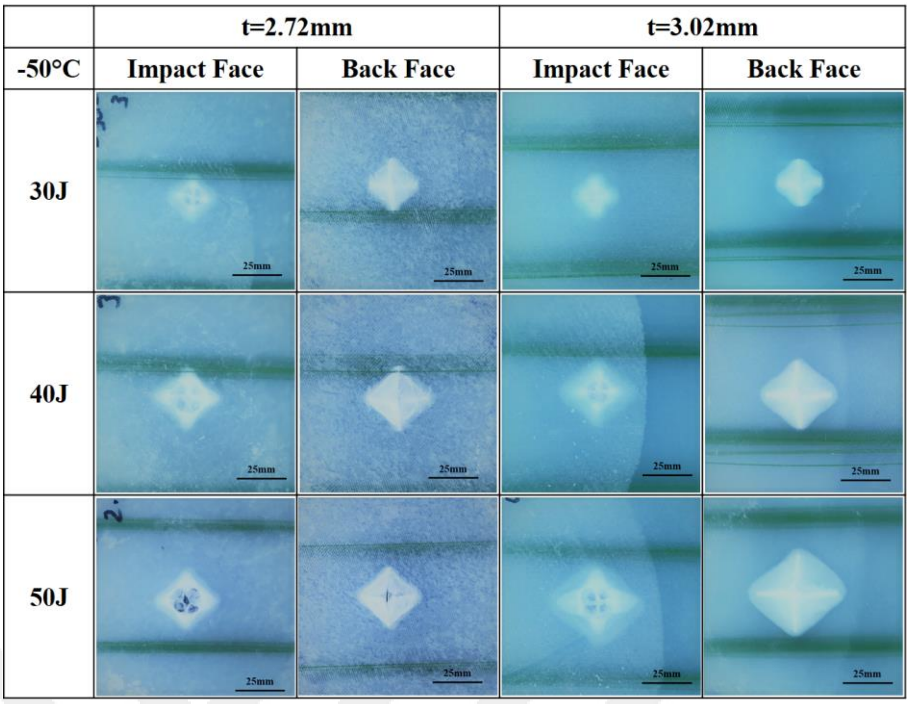

Figure 4.14 Impact damage types of S2/glass epoxy samples with 2.72mm and 3.02mm thicknesses at -50°C at different impact energies

Figure 4.15 shows the impact damage area on the back face. Graphs were drawn by taking the average of the damage area of the experiments in each experimental group. While calculating the damage area, SolidWorks program was used. In the SolidWorks program, the pictures of the back faces of the samples are scaled exactly to length 150mm and width 100mm. Then, in the program, the boundaries of the damaged area that has undergone damage were determined, and thus the area subjected to damage was calculated.

In Figure 4.15, samples with 2.72mm thickness did not penetrate the samples with 30J and 40J impact energy. Therefore, when passing from 30J to 40J impact energy, there is a rebound movement in the impactor, which causes the damage area to increase. As the samples undergo penetration at 50J impact energy, the increase in the damage area decreases when passing from 40J to 50J impact energy.

In Figure 4.15, samples with 30J, 40J and 50J impact energy in 3.02mm thickness did not penetrate and the impactor had rebound motion. Therefore, there is an increase in the damage area when moving from 30J to 40J impact energy. Likewise, when passing from 40J to 50J impact energy, the increase continues in the damage area.

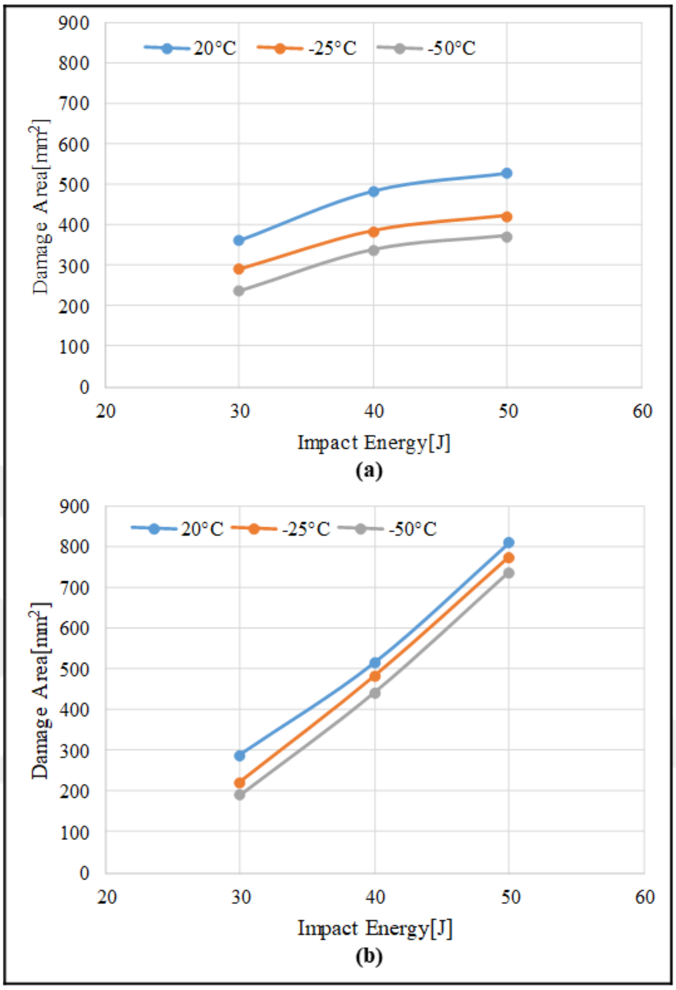

Figure 4.15 Impact damage area on the back face after low velocity impact test applied at different impact energy and temperature in samples with a) 2.72mm and b) 3.02mm thicknesses

4.2 CAI Results

CAI tests are a method used to determine the deterioration in compressive strength of a material after being subjected to impact. For this reason, CAI test was applied to samples after low velocity impact tests. The purpose of this test is to determine the change in compressive strength of samples exposed to impact at low temperatures. All samples subjected to the low velocity impact test at -50 C, -25°C and 20°C and 30J, 40J and 50J energies were subjected to the CAI test at 20°C.

CAI test results were averaged by performing at least four repetitions for each experimental group. Figure 4.16 shows the CAI test results of samples exposed to impact at 20 ° C and 30J energy for 2.72mm thickness.

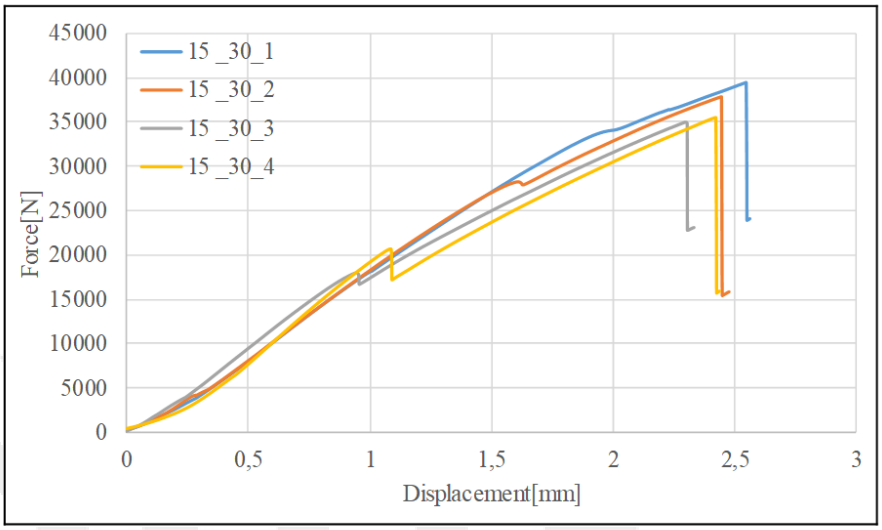

Figure 4.16 CAI test results of samples with 2.72mm thickness subjected to impact at 20°C temperature and 30J energy values

4.2.1 CAI Strength

Maximum forces and CAI strength are given in Table 4.2. When Table 4.2 is examined, it is seen that the temperature decrease and the increase in impact energy decrease the maximum force with CAI strength in samples with 2.72mm and 3.02mm thicknesses. When Table 4.2 is examined, it was observed that the samples with 2.72mm and 3.02mm thicknesses and 0J value were not damaged during the tests carried out at 20°C and they had highest CAI strength. It is observed that as the impact energy increases at 20°C, there is a decrease in CAI strength in samples of both thicknesses.

Table 4.2 Maximum forces and CAI strengths of CAI test for 2.72mm and 3.02mm thicknesses specimens subjected to low velocity impact test at different temperatures and energies

Impact Temperature	Thickness[mm]	Impact Energy[J]	Max. Force[N]	CAI Strength[MPa]
20°C	t=2.72	0	38225	140.53
		30	36975	135.94
		40	34315	126.16
		50	34108	125.40
	t=3.02	0	52158	172.71
		30	49552	164.08
		40	49043	162.39
		50	47350	156.79
-25°C	t=2.72	30	33983	124.94
		40	32909	120.99
		50	28891	106.22
	t=3.02	30	47380	156.89
		40	46800	154.97
		50	44375	146.94
-50°C	t=2.72	30	32118	118.08
		40	32037	117.78
		50	28853	106.08
	t=3.02	30	46550	154.14
		40	45296	149.99
		50	44357	146.88

The CAI strength bars were drawn as seen in Figure 4.17. When Figure 4.17 is examined, it is seen that the CAI strength also changes with the increase of impact energy at 20°C, -25°C and -50°C. The reason for this is that as the impact energy increases, the area of the damaged area on the sample increases and thus the compressive strength of the samples decreases.

When the CAI strength value is examined in the graphics, it is seen that the CAI strength increases with the increase in thickness. The reason for this can be said that the thin samples with 2.72mm thickness were exposed to more buckling during CAI test.

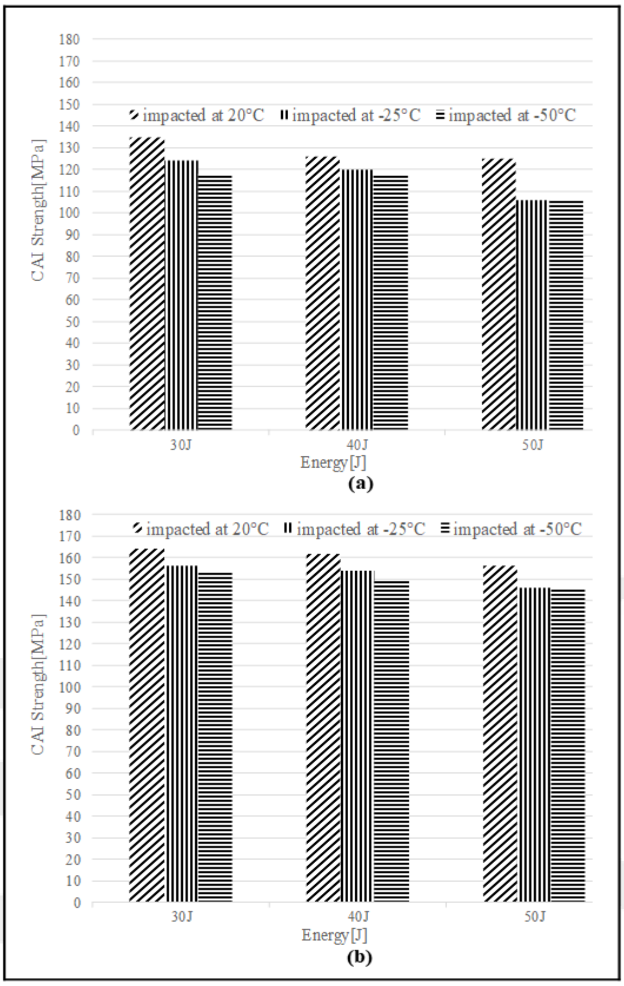

Figure 4.17 Variation of CAI strength at a) 2.72mm and b) 3.02mm thicknesses depending on temperature and energy changes

Figure 4.17 shows that the CAI strength decreases with the decrease in temperature. In the study, the results of epoxy based laminates reinforced with woven basalt fiber materials in low velocity impact tests at 25°C, -25°C and -50°C were examined. As a result, it has been observed that the stiffness of the materials increases as the temperature decreases, and as a result, the lower the temperature, the less indentation depth due to impact is examined visually. However, when the internal structure of the samples is examined using ultrasonic techniques, it is seen that the delamination between the layers increases as the temperature decreases (Ricciardi et al., 2020). Based on the results obtained, it can be said that CAI strength decreases as the temperature decreases in the tested samples.

When the samples with 2.72mm and 3.02mm thicknesses are examined in Figure 4.17, it is observed that the CAI strength results at -25°C and -50°C temperatures for 50J impact energy are very close to each other. Looking at the results, CAI strength was 106.22MPa at -25°C and 50J impact energy test for 2.72mm thickness, while CAI strength was 106.08MPa at -50°C and 50J impact energy. Similarly, CAI strength increased to 146.94MPa at -25°C and 50J for 3.02mm thickness, while CAI strength increased to 146.88MPa at -50°C and 50J. When the comparison is made according to the results, there is a slight decrease in CAI strength.

4.2.2 CAI Damage

After CAI tests, damaged samples were examined by visual inspection method. For this reason, Figure 4.18 and Figure 4.19 show the damages caused by low velocity impact test and CAI test at 20 °C of 30J, 40J and 50J impact energies of samples with 2.72mm and 3.02mm thicknesses, respectively. Figure 4.20 and Figure 4.21 show the damages of samples with 2.72mm and 3.02mm thicknesses, respectively, at -25°C for 30J, 40J and 50J impact energies, after applying low velocity impact test and CAI test. Figure 4.22 and Figure 4.23 show the damages of samples with 2.72mm and 3.02mm thicknesses for 30J, 40J and 50J impact energies at -50°C, and after applying the low velocity impact test and then CAI test.

When the samples are examined, it is seen that the majority of CAI damages begin and spread around the impact damage. The reason for the increase in CAI damage in this area can be attributed to the increase in stiffness around the damaged area. In 50J impact tests, it is seen that all samples with 2.72mm thickness are punctured at all temperature values, and complete perforation has not been observed in samples exposed to 30J and 40J impact energies. When all the figures are examined, all samples with a thickness of 3.02mm were not completely punctured at all temperatures and energy.

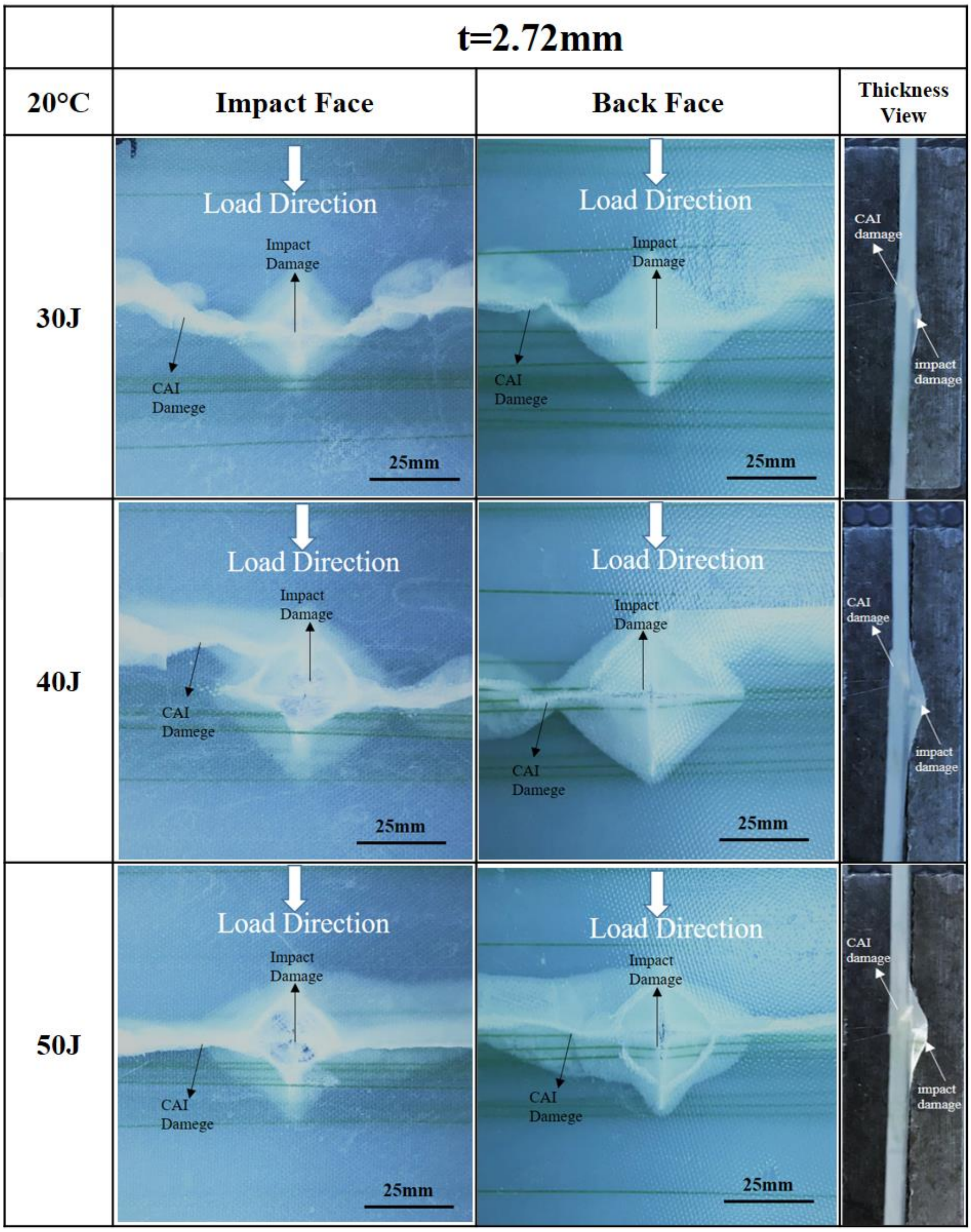

Figure 4.18 Damage after low velocity impact test and CAI test of S2 glass/epoxy samples with 2.72mm thickness at 20°C and different impact energies

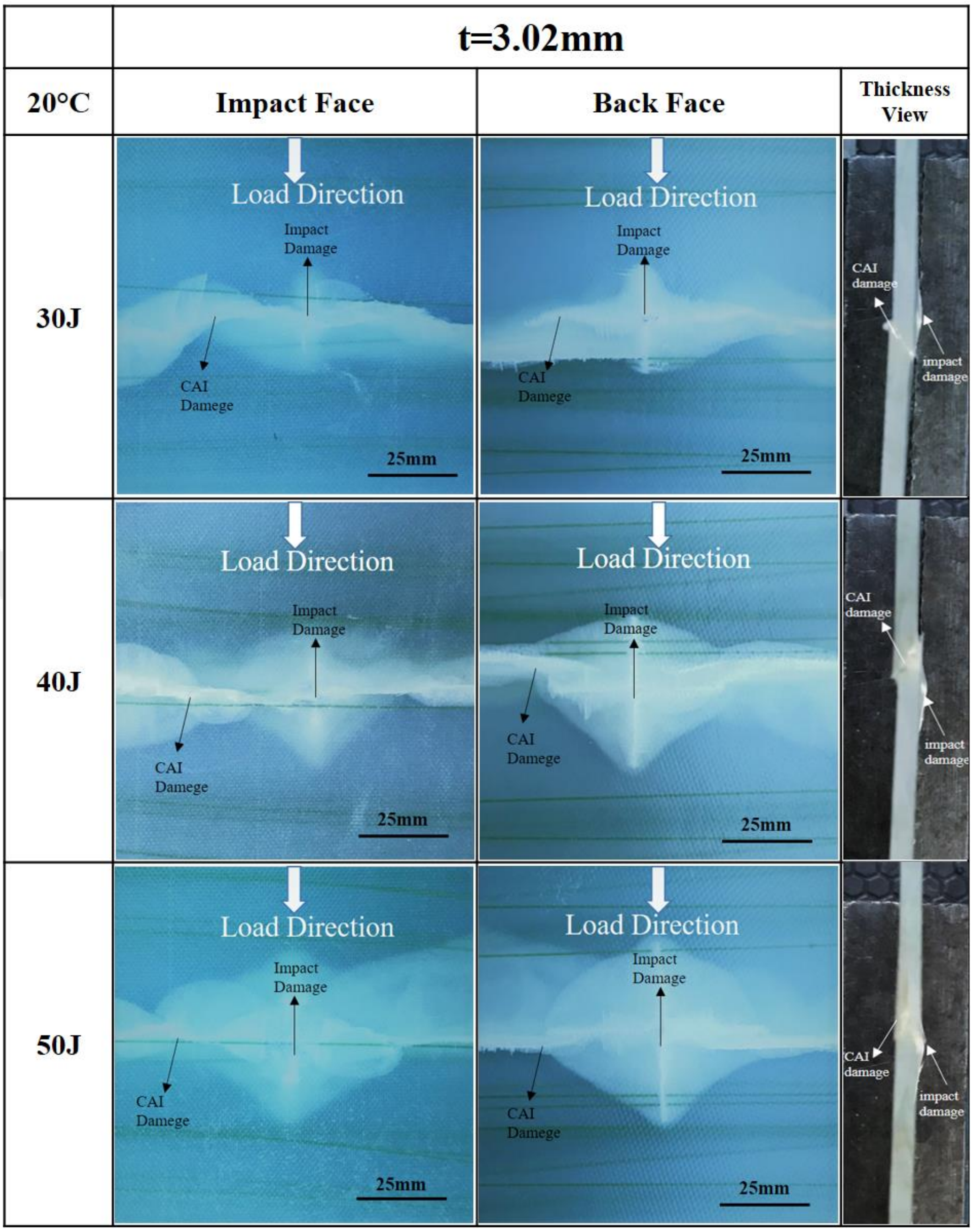

Figure 4.19 Damage after low velocity impact test and CAI test of S2 glass/epoxy samples with 3.02mm thickness at 20°C and different impact energies

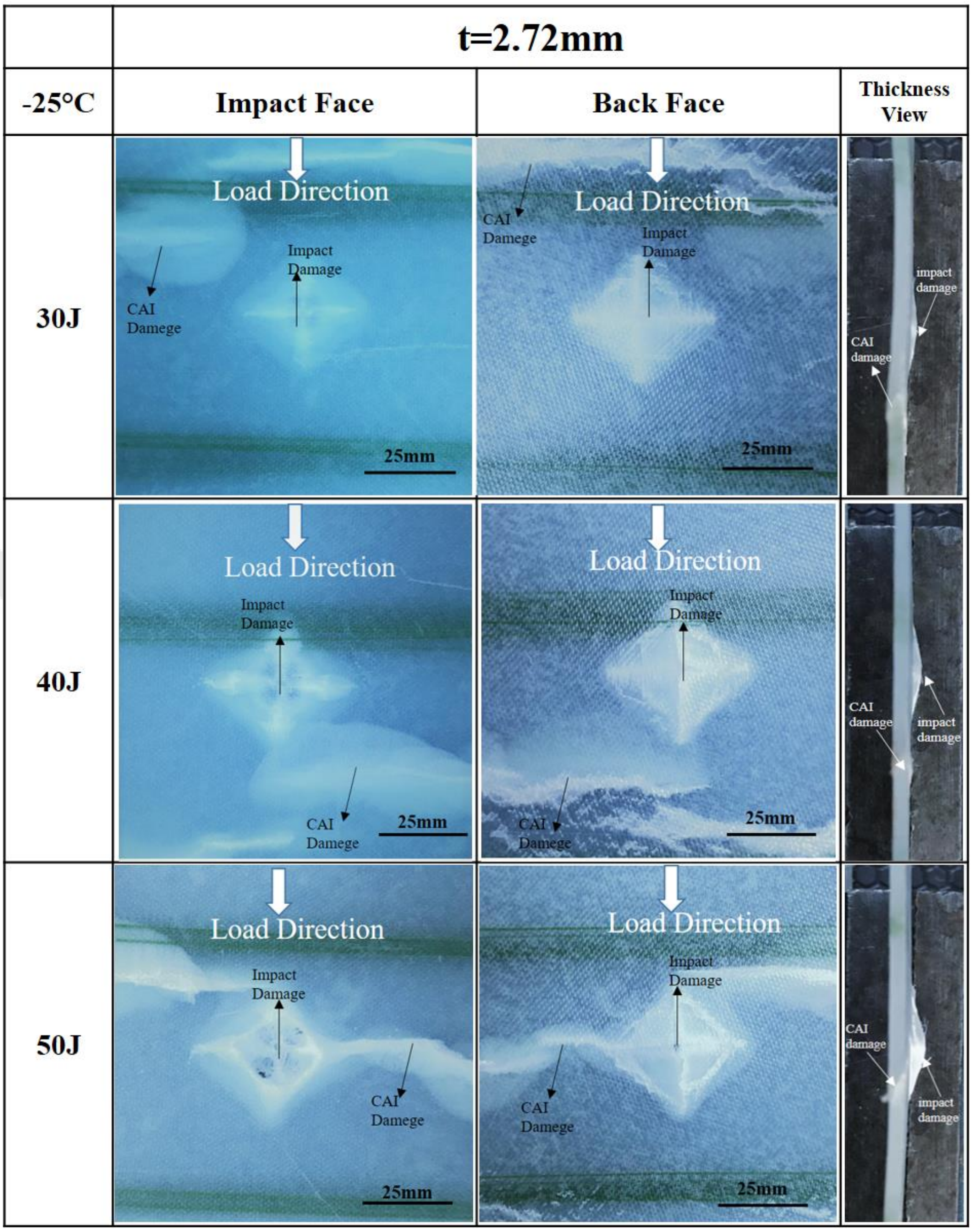

Figure 4.20 Damage after low velocity impact test and CAI test of S2 glass/epoxy samples with 2.72mm thickness at -25°C and different impact energies

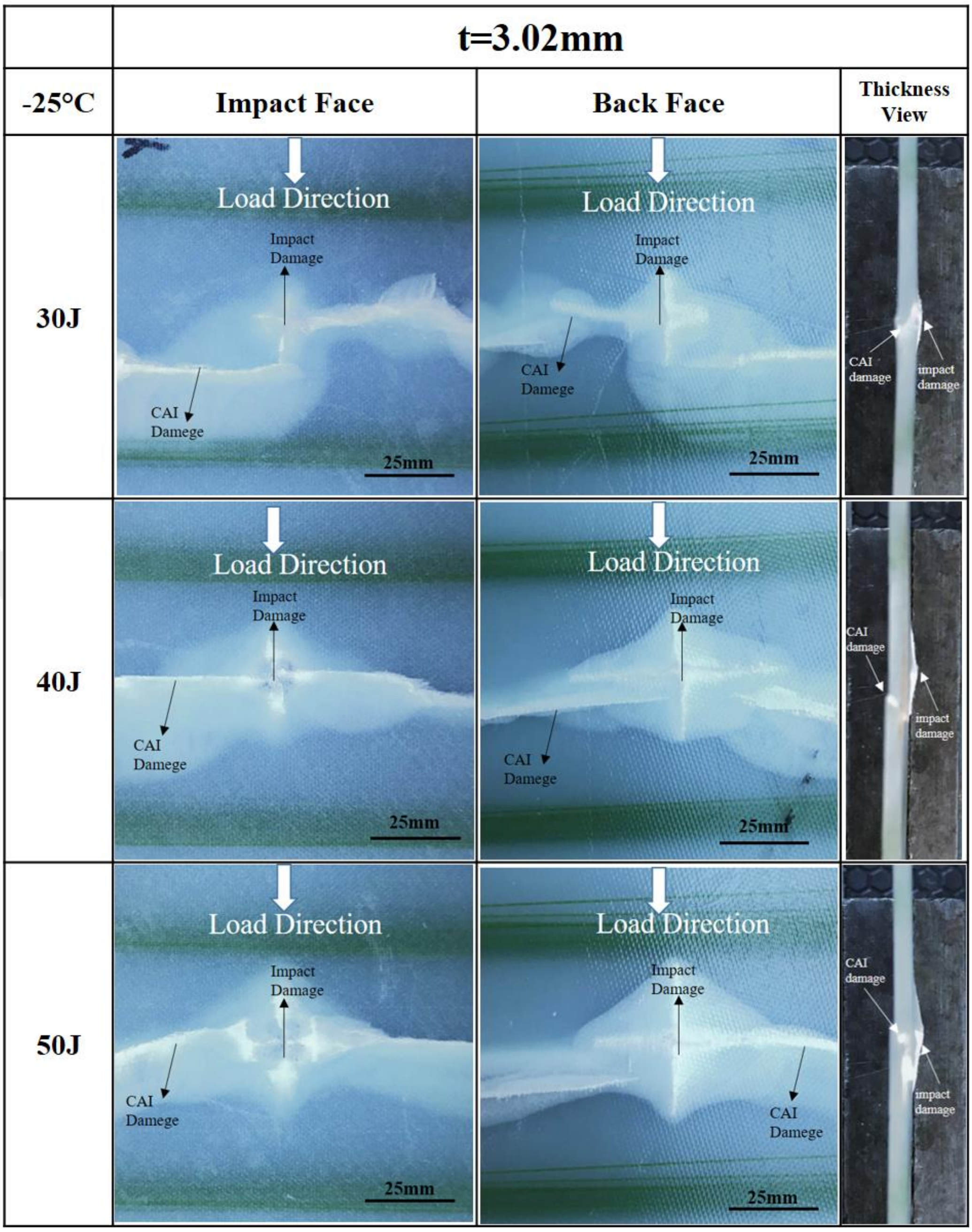

Figure 4.21 Damage after low velocity impact test and CAI test of S2 glass/epoxy samples with 3.02mm thickness at -25°C and different impact energies

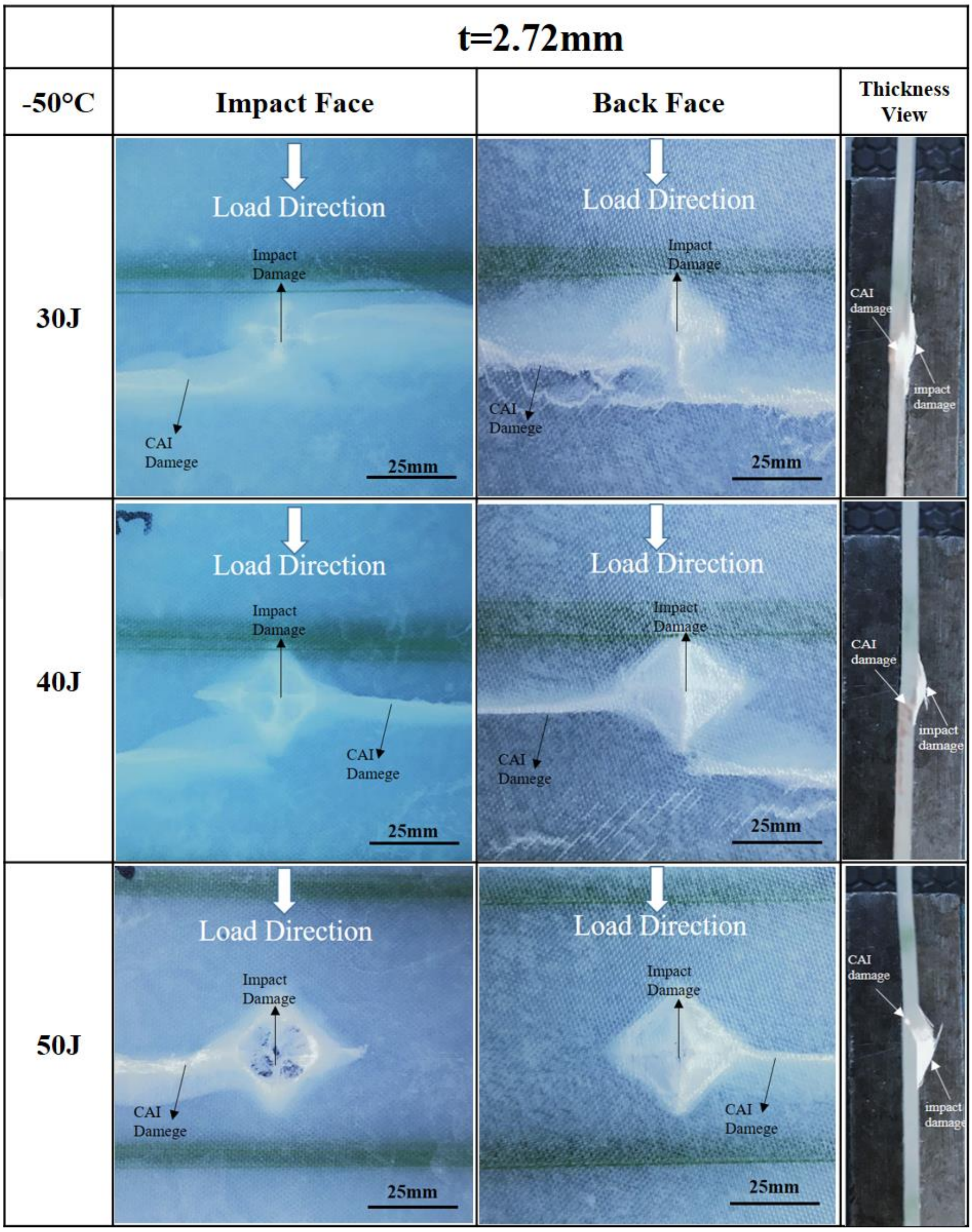

Figure 4.22 Damage after low velocity impact test and CAI test of S2 glass/epoxy samples with 2.72mm thickness at -50°C and different impact energies

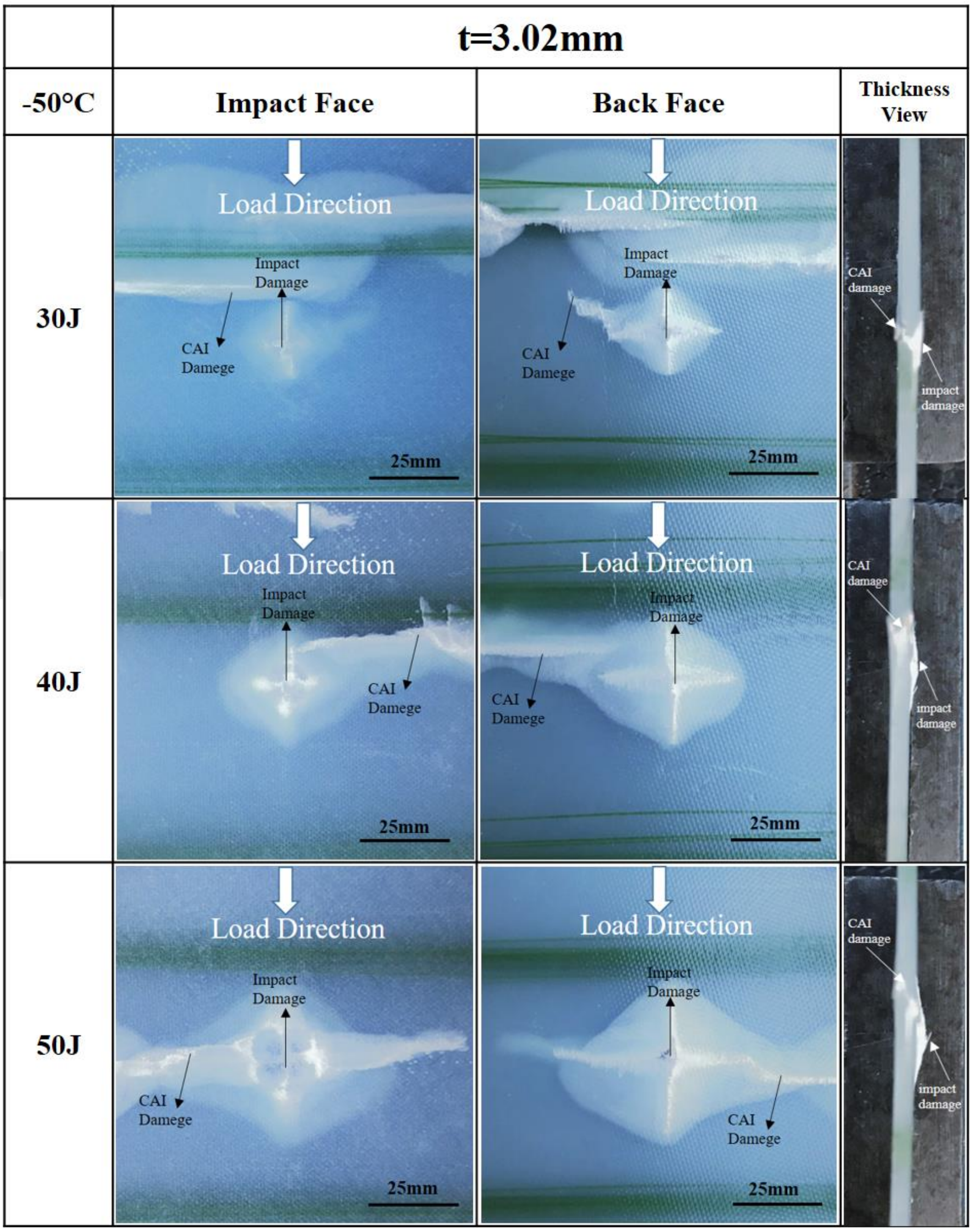

Figure 4.23 Damage after low velocity impact test and CAI test of S2 glass/epoxy samples with 3.02mm thickness at -50°C and different impact energies

CHAPTER FIVE
CONCLUSION

In this thesis, S2 glass/epoxy composites were produced by VARIM method for two different thicknesses, 2.72mm and 3.02mm. At first, low velocity impact tests were applied at 20°C, -25°C and -50°C for 30J, 40J and 50J impact energies on composite samples with the 150mm length and 100mm width. At the end of the tests, average maximum contact force, force-time and energy-time graphs were drawn for each experimental group and examined. After the low velocity impact tests, CAI tests were applied to the samples and then the compressive strength of the samples was examined. CAI tests were conducted at 20°C.

Below are the general discussion obtained after the low velocity impact tests:

- It was observed that the maximum contact force was higher in samples with 3.02mm thickness than in samples with 2.72mm thickness in the same experimental group. From this, it can be concluded that as the thickness increases, the maximum contact force increases under the same test conditions.
- The maximum contact force increased in samples with 2.72mm and 3.02mm thickness becasuse of the stiffness increase of the samples with the temperature decrease.
- The maximum contact force does not always increase with the increase of impact energy in samples with two different thicknesses in the same temperature group. The reason for this is that there may be a loss of contact between the impactor and the sample when the impactor hits the sample.
- The impact duration increases as the energy increases from 30 J to 40J at all temperatures in samples with t=2.72mm thickness. The reason for this is that when the impactor hits the sample, it bounces back and makes a rebound movement. As the energy increases, the impactor will bounce higher and the fall back time will be longer.
- The samples with 2.72mm thickness undergo full perforation at all temperatures for 50J impact energy. Therefore, these experimental groups have

the shortest duration since there is no rebound movement during the experiment.

- The impact duration increases as the impact energy increases at all temperatures in samples with 3.02mm thickness. It can be said that the reason for this is that the samples are not punctured at all temperature values and energies.
- The absorbed energy except for 40J impact energy decreased because of the decrease in temperature in samples with 2.72mm thickness. There is no significant change in the energy absorbed at 40J impact energy.
- The absorbed energy decreases and elastic energy increases with the temperature decrease in samples with 3.02mm thickness.
- The absorbed energy decreases and the elastic energy increases while the thickness of sample decreases.
- The samples with 3.02mm thickness were less damaged than the samples with 2.72mm thickness under the same test conditions.
- As the temperature decreases, there was a decrease in indentation depth in samples with 2.72mm and 3.02mm thicknesses. The reason for this is that the stiffness of the samples increases as the temperature decreases.
- With the increase in the impact energy, the damaged area of all samples are also increased for all the temperature values.
- The maximum displacement decreases as the temperature decreases in the experimental groups at the same impact energy for the samples with 2.72mm and 3.02mm thicknesses.
- In samples with 2.72mm thickness, the damage area increases in the back face of the samples for 30J and 40J impact energies. As the samples undergo penetration for 50J impact energy, the rate of increase in the damage area decreases by increase of impact energy from 40J to 50J impact energy.
- In samples with 3.02mm thickness, the damage area on the back face increases when the impact energy increases because of rebounding case.

After low velocity impact tests at 20°C, -25°C and -50°C temperatures and impact energies of 30J, 40J and 50J, CAI tests were applied to the samples at 20°C. The purpose here is to examine the increase or decrease in the compressive strength of samples impacted at different temperatures and energies. The discussion made after the CAI tests are listed below:

- The CAI strength value was higher in the samples with t=3.02mm thickness than the samples with 2.72mm thickness.
- The reason why CAI strength increases with thickness is that the samples with 2.72mm thickness buckles more compared to samples with 3.02mm thickness.
- CAI strength decreases with the increase of energy in each experiment group. The reason for this is that as the impact energy increases, the impact damage area and also the stiffness around the impact damage increase.
- CAI strength decreased with the temperature decrease for 30J, 40J and 50J impact energies in samples with 2.72mm and 3.02mm thicknesses. The reason for this is that when the samples are exposed to impact with the temperature decrease, the visible indentation depth decreases, but the damage area increases.
- CAI damage occurred around or in close proximity to the impact damage. The reason for this can be explained as, the increase in stiffness around the impact damage and the occurrence of CAI damage in this area.

With this study, it is seen the effects of thickness, impact energy and temperature change on impact response and CAI strength on S2 glass/epoxy composite material. As a recommendation for further studies, the effects of the aging method on low temperature impact response and CAI strength on S2 glass/epoxy or different laminated composites can be examined. Temperature, sample thickness, impact energy and shape of impactor nose may be an important parameter in these studies.

REFERENCES

Aktas, M., Atas, C., İçten, B.M. & Karakuzu, R. (2008). An experimental investigation of the impact response of composite laminates. *Composite Structures*, *87*, 307-313.

Aktas, M., Karakuzu, R. & Arman, Y. (2009). Compression-after impact behavior of laminated composite plates subjected to low velocity impact in high temperatures. *Composite Structures*, *89 (1)*, 77-82.

Aktas, M., Karakuzu, R. & Icten, B.M. (2010). Impact Behavior of Glass/Epoxy Laminated Composite Plates at High Temperatures. *Journal of Composite Materials*, *44 (19)*, 2289-2299.

Aktas, M., Karakuzu, R. & İçten, B.M. (2011). Thermal Impact Behavior of Glass-Epoxy-Laminated Composite Plates. *Journal of Thermoplastic Composite Materials*, *24*, 535-553.

Alpyildiz, T., Icten, B.M., Karakuzu, R. & Kurbak, A. (2009). The effect of tuck stitches on the mechanical performance of knitted fabric reinforced composites. *Composite Structures*, *89*, 391-398.

Aryal, B., Morozov, E.V., Wang, H., Shankar, K., Hazell, P.J. & Escobedo-Diaz, J.P. (2019). Effects of impact energy, velocity, and impactor mass on the damage induced in composite laminates and sandwich panels. *Composite Structures*, *226*, 111284.

Aslan, Z., Karakuzu, R. & Okutan, B. (2003). The response of laminated composite plates under low-velocity impact loading. *Composite Structures*, *59*, 119-127.

Aslan, Z., Karakuzu, R. & Sayman, O. (2002). Dynamic characteristic of laminated woven E-glass-epoxy composite plates subjected to low velocity heavy mass impact. *Journal of Composite Materials*, *36 (21)*, 2421-2442.

Atas, C. & Sayman, O. (2008). An overall view on impact response of woven fabric composite plates. *Composite Structures*, *82*, 336-345.

Bai, R., Guoa, J., Liua, Z.L.D., Maa, Y. & Yan, C. (2019). Compression after impact behavior of composite foam-core sandwich panels. *Composite Structures*, *225*, 111181.

Bienias, J., Jakubczak, P. & Dadej, K. (2016). Low velocity impact resistance of aluminium glass laminates - Experimental and numerical investigation. *Composite Structures*, *152*, 339-348.

Boumbia, R.M., Coulibaly, M., Khabouchi, A., Kinvi-Dossou, G., Bonfoh, N., Gerard, P. (2017). Glass fibres reinforced acrylic thermoplastic resin-based tri-block copolymers composites: Low velocity impact response at various temperatures. *Composite Structures, 160*, 939-951.

Campbell, F.C. (2010). *Structural composite materials* (1st ed.). Ohio: ASM International.

Galvez, V.S., Galvez, F., Cendon, D. & Sanchez, L. (2016). High-speed impact performance of carbon/epoxy composites at very low temperatures. *Procedia Engineering, 167*, 116-119.

Goren, A. & Atas, C. (2008). Manufacturing of polymer matrix composites using vacuum assisted resin infusion molding. *Archives of materials Science and Engineering, 34 (2)*, 117-120.

Han, G., Guan, Z., Li, X. & Du, S. (2016). Failure analysis of carbon fiber reinforced composite subjected to low velocity impact and compression after impact. *Journal of Reinforced Plastics and Composites, 35 (9)*, 727-746.

Icten, B.M., Atas, C., Aktas, M. & Karakuzu, R. (2009). Low temperature effect on impact response of quasi-isotropic glass/epoxy laminated plates. *Composite Structures*, *91*, 318-323.

Icten, B.M. & Karakuzu, R. (2008). Effects of Weaving Density and Curing Pressure on Impact Behavior of Woven Composite Plates. *Journal of reinforced plastics and composites*, *27 (10)*, 1083-1092.

Iqbal, K., Khan, S.U., Munir, A. & Kim, J.K. (2009). Impact damage resistance of CFRP with nanoclay-filled epoxy matrix. *Composites Science and Technology, 69*, 1949-1957.

Karakuzu, R., Erbil, E. & Aktas, M. (2010). Impact characterization of glass/epoxy composite plates: An experimental and numerical study. *Composites: Part B*, *41*, 388-395.

Kaw, A.K. (2006). *Mechanics of composite materials* (2nd ed.). Florida: CRC Press.

Kazemi, M.E., Shanmugam, L., Dadashi, A., Shakouri, M., Lu, D., Hu, D., et al. (2021). Investigating the roles of fiber, resin, and stacking sequence on the low-velocity impact response of novel hybrid thermoplastic composites. *Composites Part B, 207*, 108554.

Khashaba, U.A. & Othman, R. (2017). Low-velocity impact of woven CFRE composites under different temperature levels. *International Journal of Impact Engineering*, *108*, 191-204.

Körbelin, J., Derra, M. & Fiedler, B. (2018). Influence of temperature and impact energy on low velocity impact damage severity in CFRP. *Composites Part A*, *115*, 76-87.

Liu, H., Falzon, B.G., Tan, W. (2018). Predicting the Compression-After-Impact (CAI) strength of damage-tolerant hybrid unidirectional/woven carbon-fibre reinforced composite laminates. *Composites: Part A*, *105*, 189-202.

Mahesh, V., Joladorashi, S. & Kulkarni, S.M. (2020). Influence of laminate thickness and impactor shape on low velocity impact response of jute-epoxy composite: FE study. *Materials Today: Proceedings*, *28*, 545-550.

Mallick, P.K. (2007). *Fiber-reinforced composites: materials, manufacturing, and design*. London: CRC Press.

Ouyang, T., Bao, R., Sun, W., Guan, Z. & Tan, R. (2020). A fast and efficient numerical prediction of compression after impact (CAI) strength of composite laminates and structures. *Thin-Walled Structures, 148*, 106588.

Park, S.J. & Seo, M.K. (2011). *Interface science and composites* (1st ed.). Oxford: Elsevier.

Reddy, T. S., Mogulanna, K., Reddy, K.G., Reddy, P.R.S. & Madhu, V. (2019). Effect of thickness on behavior of E-glass/epoxy composite laminates under low velocity impact. *Procedia Structural Integrity, 14*, 265-272.

Reddy, T.S., Reddy, P.R.S. & Madhu, V. (2019). Low velocity impact studies of E-glass/epoxy composite laminates at different thicknesses and temperatures. *Defence Technology, 15*, 897-904.

Reis, P.N.B., Ferreira, J.A.M., Santos, P., Richardson, M.O.W. & Santos, J.B. (2012). Impact response of Kevlar composites with filled epoxy matrix. *Composites Structures, 94*, 3520-3528.

Reis, P.N.B, Ferreira, J.A.M., Zhang, Z.Y., Benameur, T. & Richardson, M.O.W. (2013). Impact response of Kevlar composites with nanoclay enhanced epoxy matrix. *Composites: Part B*, *46*, 7-14.

Ricciardi, M.R., Papa, I., Impera, F., Langella, A., Lapresto, V. & Antonucci, V. (2020). Low-temperature effect on the impact and flexural behaviour of basalt composite laminates. *Composite Structures*, *249*, 112607.

Rio, T.G.D., Zaera, R., Barbero, E. & Navarro, C. (2005). Damage in CFRPs due to low velocity impact at low temperature. *Composites: Part B*, *36*, 41-50.

Safir, S.N.A., Sultan, M.T.H., Jawaid, M. & Majid, M.S.A. (2019). Analysis of dynamic mechanical, low-velocity impact and compression after impact behaviour of benzoyl treated sugar palm/glass/epoxy composites. *Composite Structures*, *226*, 111308.

Salehi-Khojin, A., Bashirzadeh, R., Mahinfalah, M. & Nakhaei-Jazar, R. (2006). The role of temperature on impact properties of Kevlar/fiberglass composite laminates. *Composites: Part B*, *37*, 593-602.

Sanchez-Saez, S., Barbero, E. & Navarro, C. (2008). Compressive residual strength at low temperatures of composite laminates subjected to low-velocity impacts. *Composite Structures*, *85*, 226-232.

Shah, S.Z.H., Megat-Yusoff, P.S.M., Karuppanan, S., Choudhry, R.S., Din, I.U., Othman, A.R., et al. (2021). Compression and buckling after impact response of resin-infused thermoplastic and thermoset 3D woven composites. *Composites Part B*, *207*, 108592.

Sorrentino, L., de Vasconcellos, D.S.D, D'Auria, M., Sarasini, F. & Tirillo, J. (2017). Effect of temperature on static and low velocity impact properties of thermoplastic composites. *Composites Part B*, *113*, 100-110.

Sun, X.C. & Hallett, S.R. (2018). Failure mechanisms and damage evolution of laminated composites under compression after impact (CAI): Experimental and numerical study. *Composites: Part A*, *104*, 41-59.

Taraghi, I., Fereidoon, A., Taheri-Behrooz, F. (2014). Low-velocity impact response of woven Kevlar/epoxy laminated composites reinforced with multi-walled carbon nanotubes at ambient and low temperatures. *Materials and Design*, *53*, 152-158.

Tuo, H., Lu, Z., Ma, X., Zhang, C. & Chen, S. (2019). An experimental and numerical investigation on low-velocity impact damage and compression-after-impact behavior of composite laminates. *Composites Part B: Engineering*, *167*, 329-341.

Yang, B., Chen, Y., Lee, J., Fu, K. & Li, Y. (2021). In-plane compression response of woven CFRP composite after low-velocity impact: Modelling and experiment. *Thin-Walled Structures*, *158*, 107186.